NATIONAL ADVISORY COMMITTEE FOR AERONAUTICS

TECHNICAL NOTE

No. 1727

A SIMPLIFIED METHOD FOR THE DETERMINATION AND ANALYSIS OF THE NEUTRAL-LATERAL-OSCILLATORY-STABILITY BOUNDARY

By Leonard Sternfield and Ordway B. Gates, Jr.

Langley Aeronautical Laboratory
Langley Field, Va.

Washington
October 1948

NATIONAL ADVISORY COMMITTEE FOR AERONAUTICS

TECHNICAL NOTE NO. 1727

A SIMPLIFIED METHOD FOR THE DETERMINATION AND ANALYSIS OF THE NEUTRAL-LATERAL-OSCILLATORY-STABILITY BOUNDARY

By Leonard Sternfield and Ordway B. Gates, Jr.

SUMMARY

A necessary condition for neutral oscillatory stability is that Routh's discriminant R, formed from the coefficients of the stability equation, is equal to zero. The expression for R is $D(BC - AD) - B^2E$ where A, B, C, D, and E are the coefficients of the lateral-stability equation. In a large number of the cases considered in this study, it has been found that the term B^2E may be neglected. Routh's discriminant is then factorable into two simplified expressions, that is, $BC - AD \equiv R_1$ and D; and either $R_1 = 0$ or $D = 0$, or both, may constitute a condition of neutral stability. Test functions have been derived which, if satisfied, indicate that the simplified expressions may be used to approximate $R = 0$. If $R_1 = 0$ and $D = 0$ satisfy the necessary and sufficient conditions for a neutral-oscillatory-stability boundary, $D = 0$ represents the boundary for the oscillation which has a period comparatively longer than the period of oscillation for which $R_1 = 0$ is the boundary.

In general, the results of the computations obtained from $R_1 = 0$ and $D = 0$ show very good agreement with the results calculated by the exact expression for $R = 0$. The nature of the modes of motion as a function of the directional-stability derivative and the effective-dihedral derivative is discussed in detail.

INTRODUCTION

The results of recent investigations (references 1 and 2 and unpublished results of lateral-stability analyses for several experimental high-speed airplanes) have indicated that small variations in some of the airplane mass and aerodynamic parameters may cause a pronounced change in the oscillatory stability of the airplane. It has been difficult to explain the reasons for such pronounced changes because of the complexity of the expression for neutral oscillatory stability. This expression, based on the lateral-stability equations with three degrees of freedom, involves a large number of combinations of the mass and aerodynamic parameters. In order to predict the stability of the lateral oscillation, therefore, it appears necessary to make a separate stability analysis for each airplane.

The simplified expressions derived for the neutral-oscillatory-stability boundary in the present theoretical investigation simplify the calculations required to obtain the boundary in the analysis essential for each airplane. Because of the comparative simplicity of these expressions, an insight into the important combinations of mass and aerodynamic parameters that affect the lateral oscillatory stability is also provided. Through further investigation and analysis of the effects of these major parameters, the necessity of making separate calculations for each airplane might possibly be eliminated. Test functions are given which, if satisfied, indicate that the simplified expressions may be used.

The nature of the modes of motion as a function of C_{n_β} and C_{l_β}, the directional-stability derivative and effective-dihedral derivative, respectively, are shown to depend upon the location of the stability boundaries plotted as a function of C_{n_β} and C_{l_β}.

The results of the calculations based on the simplified expressions are presented for comparison with the results obtained by the complete expression for the neutral-oscillatory-stability boundary.

SYMBOLS AND COEFFICIENTS

ϕ	angle of bank, radians
ψ	angle of azimuth, radians
β	angle of sideslip, radians (v/V)
v	sideslip velocity along the Y-axis, feet per second
V	airspeed, feet per second
ρ	mass density of air, slugs per cubic foot
q	dynamic pressure, pounds per square foot $\left(\frac{1}{2}\rho V^2\right)$
b	wing span, feet
S	wing area, square feet
W	weight of airplane, pounds

m	mass of airplane, slugs (W/g)
g	acceleration due to gravity, feet per second per second
μ_b	relative-density factor $(m/\rho Sb)$
η	inclination of principal longitudinal axis of airplane with respect to flight path, positive when principal axis is above flight path at the nose, degrees (see fig. 1)
θ	angle between reference axis and horizontal axis, positive when reference axis is above horizontal axis, degrees (see fig. 1)
ϵ	angle between reference axis and principal axis, positive when reference axis is above principal axis, degrees (see fig. 1)
γ	angle of flight path to horizontal axis, positive in a climb, degrees (see fig. 1)
k_{X_0}	radius of gyration in roll about principal longitudinal axis, feet
k_{Z_0}	radius of gyration in yaw about principal vertical axis, feet
K_{X_0}	nondimensional radius of gyration in roll about principal longitudinal axis $\left(k_{X_0}/b\right)$
K_{Z_0}	nondimensional radius of gyration in yaw about principal vertical axis $\left(k_{Z_0}/b\right)$
K_X	nondimensional radius of gyration in roll about longitudinal stability axis $\left(\sqrt{{K_{X_0}}^2 \cos^2\eta + {K_{Z_0}}^2 \sin^2\eta}\right)$
K_Z	nondimensional radius of gyration in yaw about vertical stability axis $\left(\sqrt{{K_{Z_0}}^2 \cos^2\eta + {K_{X_0}}^2 \sin^2\eta}\right)$
K_{XZ}	nondimensional product-of-inertia parameter $\left(\left({K_{Z_0}}^2 - {K_{X_0}}^2\right) \sin \eta \cos \eta\right)$

C_L trim lift coefficient $\left(\frac{W \cos \gamma}{qS}\right)$

C_l rolling-moment coefficient $\left(\frac{\text{Rolling moment}}{qSb}\right)$

C_n yawing-moment coefficient $\left(\frac{\text{Yawing moment}}{qSb}\right)$

C_Y lateral-force coefficient $\left(\frac{\text{Lateral force}}{qS}\right)$

C_{l_β} effective-dihedral derivative, rate of change of rolling-moment coefficient with angle of sideslip, per radian $\left(\partial C_l/\partial\beta\right)$

C_{n_β} directional-stability derivative, rate of change of yawing-moment coefficient with angle of sideslip, per radian $\left(\partial C_n/\partial\beta\right)$

C_{Y_β} lateral-force derivative, rate of change of lateral-force coefficient with angle of sideslip, per radian $\left(\partial C_Y/\partial\beta\right)$

C_{n_r} damping-in-yaw derivative, rate of change of yawing-moment coefficient with yawing-angular-velocity factor, per radian $\left(\partial C_n/\partial\frac{rb}{2V}\right)$

C_{n_p} rate of change of yawing-moment coefficient with rolling-angular-velocity factor, per radian $\left(\partial C_n/\partial\frac{pb}{2V}\right)$

C_{l_p} damping-in-roll derivative, rate of change of rolling-moment coefficient with rolling-angular-velocity factor, per radian $\left(\partial C_l/\partial\frac{pb}{2V}\right)$

C_{l_r} rate of change of rolling-moment coefficient with yawing-angular-velocity factor, per radian $\left(\partial C_l/\partial\frac{rb}{2V}\right)$

C_{Y_p} rate of change of lateral-force coefficient with rolling-angular-velocity factor, per radian $\left(\partial C_Y/\partial\frac{pb}{2V}\right)$

C_{Y_r} rate of change of lateral-force coefficient with yawing-angular-velocity factor, per radian $\left(\partial C_Y/\partial\frac{rb}{2V}\right)$

t time, seconds

s_b	nondimensional time parameter based on span (Vt/b)
D_b	differential operator $\left(\frac{d}{ds_b}\right)$
R	Routh's discriminant
λ	complex root of stability equation $A\lambda^4 + B\lambda^3 + C\lambda^2 + D\lambda + E = 0 \quad (\lambda = \xi \pm i\omega)$
λ'	complex root of stability equation $\bar{A}\lambda'^4 + \bar{B}\lambda'^3 + \bar{C}\lambda'^2 + \bar{D}\lambda' + \bar{E} = 0 \quad (\lambda' = \xi' \pm i\omega')$
P	period of oscillation, seconds
$T_{1/2}$	time for amplitude of oscillation to change by factor of 2 (positive value indicates a decrease to half-amplitude, negative value indicates an increase to double amplitude)
A,B,C,D,E	coefficients of lateral-stability equation

EQUATIONS OF MOTION

The nondimensional linearized equations of motion, referred to the stability axes, used to calculate the spiral-stability and oscillatory-stability boundaries for any flight condition, are:

Rolling

$$2\mu_b\left(K_X^2 D_b^2\phi + K_{XZ}D_b^2\psi\right) = C_{l_\beta}\beta + \frac{1}{2}C_{l_p}D_b\phi + \frac{1}{2}C_{l_r}D_b\psi$$

Yawing

$$2\mu_b\left(K_Z^2 D_b^2\psi + K_{XZ}D_b^2\phi\right) = C_{n_\beta}\beta + \frac{1}{2}C_{n_p}D_b\phi + \frac{1}{2}C_{n_r}D_b\psi$$

Sideslipping

$$2\mu_b\left(D_b\beta + D_b\psi\right) = C_{Y_\beta}\beta + \frac{1}{2}C_{Y_p}D_b\phi + C_L\phi + \frac{1}{2}C_{Y_r}D_b\psi + \left(C_L \tan\gamma\right)\psi$$

When $\phi_o e^{\lambda s_b}$ is substituted for ϕ, $\psi_o e^{\lambda s_b}$ for ψ, and $\beta_o e^{\lambda s_b}$ for β in the equations written in determinant form, λ must be a root of the stability equation

$$A\lambda^4 + B\lambda^3 + C\lambda^2 + D\lambda + E = 0 \tag{1}$$

where

$$A = 8\mu_b^3\left(K_X^2K_Z^2 - K_{XZ}^2\right)$$

$$B = -2\mu_b^2\left(2K_X^2K_Z^2C_{Y_\beta} + K_X^2C_{n_r} + K_Z^2C_{l_p} - 2K_{XZ}^2C_{Y_\beta} - K_{XZ}C_{l_r} - K_{XZ}C_{n_p}\right)$$

$$C = \mu_b\left(K_X^2C_{n_r}C_{Y_\beta} + 4\mu_bK_X^2C_{n_\beta} + K_Z^2C_{l_p}C_{Y_\beta} + \frac{1}{2}C_{n_r}C_{l_p} - K_{XZ}C_{l_r}C_{Y_\beta} - 4\mu_bK_{XZ}C_{l_\beta} - C_{n_p}K_{XZ}C_{Y_\beta} - \frac{1}{2}C_{n_p}C_{l_r} + K_{XZ}C_{n_\beta}C_{Y_p} - K_Z^2C_{Y_p}C_{l_\beta} - K_X^2C_{Y_r}C_{n_\beta} + K_{XZ}C_{Y_r}C_{l_\beta}\right)$$

$$D = -\frac{1}{4}C_{n_r}C_{l_p}C_{Y_\beta} - \mu_bC_{l_p}C_{n_\beta} + \frac{1}{4}C_{n_p}C_{l_r}C_{Y_\beta} + \mu_bC_{n_p}C_{l_\beta} + 2\mu_bC_LK_{XZ}C_{n_\beta} - 2\mu_bC_LK_Z^2C_{l_\beta} - 2\mu_bK_X^2C_{n_\beta}C_L\tan\gamma + 2\mu_bK_{XZ}C_{l_\beta}C_L\tan\gamma + \frac{1}{4}C_{l_p}C_{n_\beta}C_{Y_r} - \frac{1}{4}C_{n_p}C_{l_\beta}C_{Y_r} - \frac{1}{4}C_{l_r}C_{n_\beta}C_{Y_p} + \frac{1}{4}C_{n_r}C_{l_\beta}C_{Y_p}$$

$$E = \frac{1}{2}C_L\left(C_{n_r}C_{l_\beta} - C_{l_r}C_{n_\beta}\right) + \frac{1}{2}C_L\tan\gamma\left(C_{l_p}C_{n_\beta} - C_{n_p}C_{l_\beta}\right)$$

Multiplying equation (1) by μ_b and substituting $\lambda = \frac{\lambda'}{\mu_b}$ results in the stability equation

$$\bar{A}\lambda'^4 + \bar{B}\lambda'^3 + \bar{C}\lambda'^2 + \bar{D}\lambda' + \bar{E} = 0 \tag{2}$$

where

$$\bar{A} = \frac{A}{\mu_b{}^3}$$

$$\bar{B} = \frac{B}{\mu_b{}^2}$$

$$\bar{C} = \frac{C}{\mu_b}$$

$$\bar{D} = D$$

$$\bar{E} = \mu_b E$$

The damping and period of the lateral oscillation in seconds are given respectively by the equations

$$T_{1/2} = -\frac{0.69}{\xi'}\frac{\mu_b b}{V}$$

$$P = \frac{6.28}{\omega'}\frac{\mu_b b}{V}$$

where ξ' and ω' are the real and imaginary parts of the complex root of stability equation (2).

ANALYSIS

The necessary and sufficient conditions for neutral oscillatory stability, as shown in reference 3, are that the coefficients of the stability equation satisfy Routh's discriminant set equal to zero

$$R = BCD - AD^2 - B^2E = 0 \tag{3}$$

and that B and D have the same sign. The expression for $R = 0$ can be derived by assuming that the stability equation has two roots $\lambda = \pm i\omega$, where ω is the angular frequency of the neutrally stable oscillation. This assumption is based on the fact that for the condition of neutral oscillatory stability the real part of the complex root must be zero. If $\lambda = i\omega$ is substituted in the stability equation, the following two equations are obtained:

$$A\omega^4 - C\omega^2 + E = 0 \tag{4}$$

$$-B\omega^3 + D\omega = 0 \tag{5}$$

Solving equation (5) for ω^2 and then substituting the result $\left(\omega^2 = \frac{D}{B}\right)$ in equation (4) results in Routh's discriminant

$$BCD - AD^2 - B^2E = 0$$

It is seen from equation (5) that $\omega = \sqrt{\frac{D}{B}}$ is the angular frequency of the neutrally stable oscillation only when B and D are of the same sign since ω must have a real value if the root $\lambda = \pm i\omega$ is to represent an oscillation. If B and D are of opposite sign and $R = 0$ is satisfied, the two roots of the stability equation given by $\lambda = \pm i\omega$ are real, one positive and one negative. It is important to note that the A, C, and E coefficients may be of opposite sign to the B and D coefficients, and neutral oscillatory stability will still occur as long Routh's discriminant is equal to zero and the D and B coefficients are of the same sign.

In general, the $R = 0$ boundary in the C_{n_β},C_{l_β} plane has two branches. The two branches result from the fact that $R = 0$ is a quadratic equation in C_{l_β} and thus has two C_{l_β} roots for every value of C_{n_β}. Usually, the two branches can be approximated by simplified expressions for $R = 0$. In certain cases, however, which are discussed in the section entitled "Test Functions," either one or none of the branches may be approximated.

Now, the condition $R = 0$ is a necessary but insufficient condition for neutral oscillatory stability. The simplified expressions, therefore, which approximate $R = 0$ do not necessarily represent boundaries of neutral oscillatory stability. Other conditions, elaborated on in the section "Validity of $D = 0$ and $R_1 = 0$ as Neutral-Oscillatory-Stability Boundaries," must be satisfied before either expression represents a valid boundary.

There are, therefore, two kinds of tests that must be made: First, tests to determine whether $R = 0$ may be approximated by simplified expressions; and, second, tests to determine which of these expressions represents a boundary of neutral oscillatory stability. The significance of the lateral-stability boundaries is indicated by a discussion of the modes of motion in the C_{n_β},C_{l_β} plane.

Derivation of Simplified Expressions

Two of the most important stability derivatives affecting lateral oscillatory stability are the directional-stability derivative C_{n_β} and the effective-dihedral derivative C_{l_β}. The boundary for neutral oscillatory stability is usually plotted as a function of these two derivatives with C_{n_β} as the ordinate and C_{l_β} as the abscissa. The method used to obtain the neutral oscillatory stability boundary is first to substitute the values of the mass and aerodynamic parameters of a specific airplane in the coefficients of the stability equation while maintaining C_{n_β} and C_{l_β} as variables and then to calculate the C_{l_β} roots of equation (3) for several values of C_{n_β}. For a given value of C_{n_β}, the expression for $R = 0$ is a quadratic equation in C_{l_β} that is of the form

$$a_1 C_{l_\beta}^{\ 2} + b_1 C_{l_\beta} + c_1 = 0$$

For a very large number of cases, it has been found that the last term of Routh's discriminant B^2E, which contributes only to b_1 and c_1, produces a negligible change in the expression

$$a_1 C_{l_\beta}{}^2 + b_1 C_{l_\beta} + c_1 = 0$$

If, therefore, the term B^2E is neglected, equation (3) for Routh's discriminant reduces to

$$R = D(BC - AD) = 0 \tag{6a}$$

Thus $BC - AD = 0$ and $D = 0$ are the approximate factors of the quadratic equation

$$a_1 C_{l_\beta}{}^2 + b_1 C_{l_\beta} + c_1 = 0$$

The expression $BC - AD$ is henceforth called R_1.

In order to simplify the expressions for R_1 and D, the expected range of values of mass and aerodynamic parameters for high-speed aircraft were substituted in the coefficients of the stability equation to determine which terms could be omitted without appreciably affecting the values of R_1 and D. The following simplified coefficients were obtained:

$$A = 8\mu_b{}^3\left(K_X{}^2K_Z{}^2 - K_{XZ}{}^2\right)$$

$$B = -2\mu_b{}^2\left(K_X{}^2C_{n_r} + 2K_X{}^2K_Z{}^2C_{Y_\beta} + C_{l_p}K_Z{}^2\right)$$

$$C = \mu_b\left(4\mu_bK_X{}^2C_{n_\beta} - 4\mu_bK_{XZ}C_{l_\beta} + \frac{1}{2}C_{n_r}C_{l_p} + C_{l_p}K_Z{}^2C_{Y_\beta} - \frac{1}{2}C_{n_p}C_{l_r}\right)$$

$$D = \mu_b\left(C_{n_p} - 2C_LK_Z{}^2\right)C_{l_\beta} - \mu_b\left(C_{l_p} - 2C_LK_{XZ}\right)C_{n_\beta}$$

$$E = \frac{1}{2} C_L\left(C_{n_r}C_{l_\beta} - C_{l_r}C_{n_\beta}\right)$$

The expressions for R_1 and D thus become

$$R_1 = \left(A_1K_{XZ} - A_2A_3\right)C_{l_\beta} + \left[-K_{XZ}\left(2A_3C_L + C_{l_p}K_{XZ}\right) - K_X{}^2\left(A_1 - C_{l_p}K_Z{}^2\right)\right]C_{n_\beta}$$
$$- \frac{A_1}{8\mu_b}\left[\frac{C_{l_p}}{K_X{}^2}\left(A_1 - C_{l_p}K_Z{}^2\right) - C_{l_r}C_{n_p}\right] = 0 \tag{6b}$$

and

$$D = A_2C_{l_\beta} - \left(C_{l_p} - 2C_LK_{XZ}\right)C_{n_\beta} = 0 \tag{6c}$$

where

$$\left.\begin{aligned} A_1 &= K_X{}^2C_{n_r} + 2K_X{}^2K_Z{}^2C_{Y_\beta} + C_{l_p}K_Z{}^2 \\ A_2 &= C_{n_p} - 2C_LK_Z{}^2 \\ A_3 &= K_X{}^2K_Z{}^2 - K_{XZ}{}^2 \end{aligned}\right\} \tag{6d}$$

The simplified expressions $R_1 = 0$ and $D = 0$, as presented, are applicable only to conditions of level flight or to conditions of small angles of glide or climb. Simplified expressions for conditions of large angles of glide or climb can be derived by a procedure similar to the one presented.

Test Functions

The approximate discriminants $R_1 = 0$ and $D = 0$ are based on the assumption that B^2E can be neglected when Routh's discriminant is set equal to zero. Thus, the simplified expressions for the neutral-oscillatory-stability boundary, R_1 and D, should not be used if including the terms B^2E causes an appreciable change in the roots of $R = 0$. In appendix A test functions are derived which indicate the incremental change in the roots of $R_1 = 0$ and $D = 0$ due to the terms B^2E. If certain conditions placed upon these test functions are satisfied, then R_1 and D can be used to calculate the $R = 0$ boundary.

If, at a given value of C_{n_β}, the root of $R_1 = 0$ is denoted by $C_{l_\beta} = r$, the approximate deviation of this root from a root of $R = 0$ is given by

$$\Delta r = \frac{e_1(e - r)}{r_1 d_1(d - r) + e_1} \tag{7}$$

If Δr is small, then $R_1 = 0$ is a close approximation to one branch of $R = 0$. A suitable criterion for this approximation is

$$\left|\Delta r\right| \leqq \left|\frac{r}{5}\right|$$

or

$$\left|\Delta r\right| \leqq 0.01$$

whichever is the larger.

Similarly if a root of $D = 0$ is denoted by $C_{l_\beta} = d$, the approximate deviation of this root from a root of $R = 0$ is given by

$$\Delta d = \frac{e_1(e - d)}{r_1 d_1(r - d) + e_1} \tag{8}$$

If Δd is small, then $D = 0$ is a close approximation to one branch of of $R = 0$. A suitable criterion for this approximation is

$$\left|\Delta d\right| \leqq \left|\frac{d}{5}\right|$$

or

$$\left|\Delta d\right| \leqq 0.01$$

whichever is the larger.

The expressions for r_1, d_1, e_1, r, d, and e for use in equations (7) and (8) are

$$r_1 = 8\mu_b\left(A_1K_{XZ} - A_2A_3\right)$$

$$d_1 = \mu_bA_2$$

$$e_1 = 2\mu_bA_1{}^2C_LC_{n_r}$$

$$r = \left(C_{l_\beta}\right)_{R_1=0}$$

$$d = \left(C_{l_\beta}\right)_{D=0}$$

$$e = \left(C_{l_\beta}\right)_{B^2E=0}$$

where A_1, A_2, and A_3 are defined in equations (6d).

The value of C_{n_β} to be used in these test functions should be selected from the probable range of C_{n_β} of the airplane for which the lateral-stability analysis is to be made. Thus, the approximation of $R_1 = 0$ and $D = 0$ to $R = 0$ is determined in that region of the C_{n_β},C_{l_β} plane pertinent to a particular analysis.

Validity of $D = 0$ and $R_1 = 0$ as Neutral-Oscillatory-Stability Boundaries

As mentioned previously, for $R = 0$ to be a boundary for neutral oscillatory stability, the coefficients B and D must be of the same sign. The three predominant terms of B contain the factors $-C_{n_r}$, $-C_{Y_\beta}$, and $-C_{l_p}$, respectively. For positive damping in roll, C_{l_p}

is negative; and for positive weathercock stability $\left(C_{n_\beta}\text{ positive}\right)$, C_{Y_β} and C_{n_r} are negative. Thus, B is positive in the usual case where there is weathercock stability and damping in roll. Therefore, D must generally be positive in order that $R = 0$ be a neutral-stability boundary. If the exact boundary $R = 0$ has been calculated, it is merely necessary to plot $D = 0$ and $R = 0$ and note whether $R = 0$ is located on the side of $D = 0$ where D is positive. A primary purpose of the present paper, however, is to obviate calculation of the exact boundary by the use of simplified boundaries together with test functions. A method to determine the sign of D from the results of the simplified expressions is therefore presented in the following paragraph.

For a given value of C_{n_β} $\left(\text{selected from the probable range of } C_{n_\beta}\text{ of the airplane for which the lateral-stability analysis is to be made}\right)$ let d be a value of C_{l_β} for which $D = 0$ and d' be a slightly different value for which $R = R_1D - B^2E = 0$. The substitution of $C_{l_\beta} = d'$ gives

$$D(d') = \frac{B^2E(d')}{R_1(d')}$$

The sign of D at the $R = 0$ boundary $\left(C_{l_\beta} = d'\right)$ is therefore determined by the signs of E and R_1 at d'. But since d differs little from d', the signs of E(d) and $R_1(d)$ will be the same as the signs of E(d') and $R_1(d')$, respectively. Hence the sign of D at $R = 0$ is the same as the sign of E/R_1 at $D = 0$ (fig. 2); that is,

$$D(d') = \frac{E(d)}{R_1(d)}$$

If the signs of E and R_1 are the same, D is positive and represents a neutral-oscillatory-stability boundary; if E and R_1 are of opposite sign, D is negative and then represents a boundary for which the roots of the stability equation are equal and opposite in sign.

The preceding analysis is applicable for the large majority of cases where E(d') and $R_1(d')$ are of the same sign as E(d) and $R_1(d)$, respectively. For these cases, the D curve is widely separated from the E and R_1 curves. If the D curve is close to either the E or R_1 curve, the signs of E and R_1 should be determined at $C_{l_\beta} = d'$. However, a very good approximation to the value of d' can be obtained by adding to d the value of Δd calculated in the previous section entitled "Test Functions." Hence, the sign of D is determined from the signs of E and R_1 at $C_{l_\beta} = d + \Delta d$.

If the value of C_{l_β} at which $R_1 = 0$ is substituted in D and the resultant sign is positive, $R_1 = 0$ is a neutral-oscillatory-stability boundary.

It is interesting to note that for some aircraft, the $D = 0$ curve, which approximates one branch of the $R = 0$ curve, is a neutral-oscillatory-stability boundary over one section of the curve and a boundary for equal and opposite real roots over the remaining section. This division of the $D = 0$ curve into two distinct parts is caused by a change in sign of the D coefficient at some point on the curve. If, as has been found in a large number of cases, R_1 is positive for all values of C_{n_β} and C_{l_β} on the $D = 0$ curve, the sign of the D coefficient depends only on the sign of E at these points. As shown in figure 3, therefore, the point of intersection of the curves $D = 0$ and $E = 0$ is the point of separation of the $D = 0$ curve into two characteristically different sections. For points on the hatched side of $E = 0$, the E coefficient is negative and, therefore, the dashed part of $D = 0$ is a boundary of equal and opposite real roots. Conversely, on the unhatched side of $E = 0$, the E coefficient is positive and the solid part of $D = 0$ approximates a boundary of neutral oscillatory stability.

For small positive or negative values of C_{n_β} and negative damping in roll, it is possible for B to be negative. A similar analysis is applicable to this case where now D must be negative to satisfy the necessary condition that $R = 0$ is a boundary of neutral oscillatory stability.

In general, when the simplified expressions are used to obtain a neutral-oscillatory-stability boundary, the procedure to be used is as follows:

(1) For a given value of C_{n_β}, selected from the probable range of C_{n_β} of the airplane for which the lateral-stability analysis is to be made, calculate r and d, the C_{l_β} roots of $R_1 = 0$ and $D = 0$, respectively.

(2) Determine the value of Δr and Δd by substituting the results into the test functions.

(3) If the criterions for Δr and Δd as set forth in appendix A are satisfied, consider $R_1 = 0$ and $D = 0$ close approximations to the $R = 0$ boundary.

(4) In order to determine the validity of $R_1 = 0$ as a boundary of neutral oscillatory stability, substitute the given value of C_{n_β} and $C_{l_\beta} = r$ into the D coefficient. (If the resulting sign is positive, $R_1 = 0$ approximates a branch of the neutral-oscillatory-stability boundary.)

(5) In order to determine the validity of $D = 0$ as a boundary of neutral oscillatory stability, substitute the given value of C_{n_β} and $C_{l_\beta} = d$ into $\frac{E}{R_1}$. (If the resulting sign is positive, $D = 0$ approximates a branch of the neutral-oscillatory-stability boundary; if the resulting sign is negative, $D = 0$ approximates a boundary of equal and opposite real roots.)

Nature of Modes of Motion in the C_{n_β}, C_{l_β} Plane

In this section, the changes in the roots of the lateral-stability equation, which occur upon crossing the various stability boundaries, are discussed according to the principles of the theory of equations as given in references 3 and 4. The solution of the lateral-stability equation gives four roots which may be four real roots, two pairs of conjugate complex roots, or two real roots and one conjugate complex pair. A pair of complex roots indicates an oscillatory mode and a real root indicates an aperiodic mode. If the airplane is disturbed from its trimmed condition by an arbitrary disturbance, the subsequent motion is compounded of these modes in different proportions. The method of calculating the different proportions of the modes is presented, for example, in references 5 and 6. Such calculations of the motion for numerous points throughout the C_{n_β}, C_{l_β} plane would be very laborious. It is more practical, therefore, to investigate merely the types of modes that may be expected throughout the C_{n_β}, C_{l_β} plane as indicated by the stability boundaries. The calculation of the motion could then be limited to several points of interest.

Consider a case where the neutral-oscillatory-stability boundary $R_1 = 0$ and the spiral-stability boundary $E = 0$ are located in the first quadrant of figure 4(a). The area between the two boundaries is a region of complete stability. The roots of the stability equation for combinations of C_{n_β} and C_{l_β} in this region, such as point A in figure 4(a), are two negative real roots and one conjugate complex pair with the real part negative. One of the real roots which is numerically small corresponds to the spirally stable motion of the airplane. The other real root corresponds to the heavy damping of the pure rolling motion. The complex roots with the real part negative show that the so-called Dutch roll oscillation is stable. Passing through the $E = 0$ boundary from point A to point B causes the spiral mode to become unstable, and crossing through the $R_1 = 0$ boundary from point A to point C causes the oscillatory mode to become unstable. The second branch of the $R = 0$ boundary plotted in the second quadrant as $D = 0$ is not a neutral-oscillatory-stability boundary but rather a boundary for equal and opposite roots as determined by the analysis presented in the section entitled "Validity of $D = 0$ and $R_1 = 0$ as Neutral-Oscillatory-Stability Boundaries." The roots of the stability equation for combinations of C_{n_β} and C_{l_β} on this boundary are two equal and opposite real roots and a pair of complex roots with the real part negative. The positive real root is the spirally unstable mode, and the negative real root is the damping-in-roll mode. The oscillation continues to remain stable even though the D coefficient is negative.

For the case where one oscillatory-stability boundary $D = 0$ appears in the first quadrant and another oscillatory stability boundary $R_1 = 0$ is in the second quadrant, (fig. 4(b)), the period of the neutrally stable oscillation is much greater on $D = 0$ than on $R_1 = 0$. This fact can be shown to be true by investigating the angular frequency of the neutrally stable oscillation for points located on the $R_1 = 0$ and $D = 0$ boundaries. As shown previously, the angular frequency ω is equal to $\sqrt{D/B}$; and, therefore, since the boundary $D = 0$ approximates one branch of $R = 0$, the angular frequency for points on that branch is very small. For combinations of C_{n_β} and C_{l_β} on $R_1 = 0$, the angular frequency is much greater. In general, $D = 0$ is a neutral-oscillatory-stability boundary for a long-period oscillation. The roots at point A of figure 4(b) have the same character as the roots at point A of figure 4(a), that is, two negative real roots and one pair of conjugate complex roots. At point B the roots of the lateral-stability equation are two pairs of conjugate complex roots. It is interesting to note that the boundary for two equal roots occurs between point A and point B and can be considered the boundary beyond which two pairs of complex roots exist. Reference 4 shows that for a quartic equation

$$A\lambda^4 + B\lambda^3 + C\lambda^2 + D\lambda + E = 0$$

the boundary for equal roots is obtained by setting the discriminant

$$-4P^3 - 27Q^2$$

equal to zero, where

$$P = BD - 4AE - \frac{C^2}{3}$$

and

$$Q = -B^2E + \frac{BCD}{3} + \frac{8ACE}{3} - AD^2 - \frac{2C^3}{27}$$

Between this boundary and $D = 0$, the period of the stable oscillation which corresponds to the newly formed pair of complex roots is longer than the period of the oscillation which corresponds to the other pair of complex roots. As C_{l_β} is increased to point C on the unstable side of $D = 0$, the newly formed long-period oscillation is the one that becomes unstable whereas the short-period oscillation remains stable. At point D the roots consist of a spirally unstable mode, a stable mode due to the derivative C_{l_p}, and a stable oscillation which becomes unstable in passing through $R_1 = 0$ to point E.

Figure 4(c) represents the case where both $R_1 = 0$ and $D = 0$ appear in the first quadrant but only R_1 is a neutral-oscillatory-stability boundary. The curve $D = 0$ is the boundary for two equal and opposite real roots. Point A once again has two real negative roots and a pair of complex roots with the real part negative. At point B, on the unstable side of $R_1 = 0$, the real part of the complex roots is positive and indicates an unstable oscillation, whereas the two real roots are still negative. The boundary for $C = 0$ is between $R_1 = 0$ and $D = 0$. Some investigators of lateral stability have thought that a radical change occurs in the roots upon crossing through this boundary. The calculations indicate, however, that the roots do not vary appreciably upon passing through $C = 0$. At $D = 0$, however, there must exist two equal and opposite real roots; this condition is possible only if the complex roots divide into real roots since the other two real roots are negative in sign. The calculation of roots at point C indicate that the complex roots had divided into two real positive roots, one of which was exactly equal in magnitude to one of the negative roots. Again, the boundary for two equal roots, located between $C = 0$ and point C, would determine the combination of C_{n_β} and C_{l_β} where the complex roots divide into two real roots.

There have been several cases for which a neutral-oscillatory-stability boundary did not exist in the C_{n_β}, C_{l_β} plane. An analysis of these cases indicated that the boundary for equal roots was in the oscillatorily stable region and had divided the stable oscillation into two subsiding modes. The neutral-oscillatory-stability boundary, therefore, would not have any significance.

RESULTS AND DISCUSSION

The simplified expressions were used to calculate $R_1 = 0$ and $D = 0$, and the results are compared with the results of the calculation of $R = 0$ based on the complete expression. Not only do $R_1 = 0$ and $D = 0$ show good agreement with $R = 0$ (figs. 5 to 13) but the comparative simplicity of the R_1 and D expressions allows identification of the major parameters that affect the stability boundaries.

Effect of $C_{n_p} - 2C_L K_Z^2$ on the Branch of $R = 0$ Approximated by $D = 0$

Reference 2 shows that a stabilizing shift in the $R = 0$ boundary is obtained when C_{n_p} is increased in a positive direction up to a certain value, but further increases in the positive direction cause a destabilizing shift in $R = 0$. The effect of varying C_{n_p} on the $R = 0$ curve is presented in figure 5 for a model tested in the Langley free-flight tunnel. The figure illustrates very good agreement between $R = 0$ and the simplified expressions $R_1 = 0$ and $D = 0$. The expression for $D = 0$ is

$$C_{l_\beta} = \frac{\left(C_{l_p} - 2C_L K_{XZ}\right)C_{n_\beta}}{C_{n_p} - 2C_L K_Z^2}$$

which indicates that for positive C_{n_β} when the numerator is negative in sign, the $D = 0$ boundary is in the second quadrant for negative values of $C_{n_p} - 2C_L K_Z^2 \equiv A_2$ and in the first quadrant for positive values of A_2. For the cases of negative A_2 presented in figure 5, the $D = 0$ boundary would appear in the second quandrant. It can be shown, however, by the method described in the section "Validity of $D = 0$ and $R_1 = 0$ as Neutral-Oscillatory-Stability Boundaries" that $D = 0$ in the second quadrant is not a neutral-oscillatory-stability boundary and hence is not plotted in figure 5. However, as C_{n_p} is increased in a positive direction, where now A_2 is positive, an increase in the positive value of A_2 causes the $D = 0$ boundary to shift upward in the first quadrant in a destabilizing direction.

From the results shown in figure 5, it is seen that for the cases of C_{n_p} equal to 0.30 and 0.40 only the solid-line part of the $R = 0$ curve in the first quadrant (the branch which may be approximated by $D = 0$) is a neutral-oscillatory-stability boundary. The short-dash-line part of $R = 0$ is a boundary of equal and opposite real roots. The reason for this division of the $R = 0$ curve into two parts is discussed in the section entitled "Validity of $D = 0$ and $R_1 = 0$ as Neutral-Oscillatory-Stability Boundaries" and is illustrated in figure 3.

Effect of $C_{n_p} - 2C_L K_Z^2$ on the Branch of $R = 0$ Approximated by $R_1 = 0$

The important effect of C_{n_p} on $R_1 = 0$ occurs only in the coefficient of the C_{l_β} term, $A_1 K_{XZ} - A_2 A_3$, in which C_{n_p} affects only the factor A_2. The sign of A_3 is always positive and the sign of A_1 is negative for positive C_{n_β}. By definition, K_{XZ} is positive if the principal axis is above the flight path at the nose of the airplane as is the case for the curves presented in figure 5. In general, for positive C_{n_β}, the expression of $R_1 = 0$ which does not include any C_{l_β} terms is positive and, except for one term, is independent of C_{n_p}. If, therefore, the coefficient of C_{l_β} is positive, $R_1 = 0$ is in the first quadrant; whereas if the coefficient of C_{l_β} is negative, $R_1 = 0$ is in the second quadrant. As C_{n_p} increases in a positive direction and A_2 becomes more positive, the coefficient of C_{l_β} becomes more negative and $R_1 = 0$ in the second quadrant shifts upward in a destabilizing direction. If A_2 is negative but the absolute value of A_2 increases, as in going from $C_{n_p} = 0.15$ to $C_{n_p} = -0.10$ in figure 5, the coefficient of C_{l_β} becomes more positive and R_1 in the first quadrant also shifts upward in a destabilizing direction. Thus the results indicate that increasing the absolute value of A_2 has a destabilizing effect on the neutral-oscillatory-stability boundary.

According to a previous discussion herein, variations in C_{n_p} that maintain A_2 constant cause no shift in the $D = 0$ boundary. When, therefore, $R = 0$ is approximated by $D = 0$, such changes in C_{n_p} and K_Z should have a negligible effect on the $R = 0$ boundary. In order to test this point, calculations were made for a free-flight airplane model for C_{n_p} varying from 0.30 to 0.63 while simultaneously varying $K_Z{}^2$ in order to maintain the same positive value of A_2. The results showed the expected insensitivity of the $R = 0$ boundary to these changes.

It should be remembered that $D = 0$ in the first quadrant is the neutral-oscillatory-stability boundary for the long-period oscillation; and if instability were to occur, the pilot might not find this type of instability difficult to control.

Effect of C_{n_r}, C_{Y_β}, and K_X on the Branch of $R = 0$ Approximated by $D = 0$

The D expression indicates that the $D = 0$ boundary is independent of the derivatives C_{n_r} and C_{Y_β} and the mass parameter K_X. Figures 6 and 7 show a comparison of the results obtained by the complete calculations with $D = 0$ for the cases in which C_{n_r} and C_{Y_β}, respectively, were arbitrarily doubled in value. As noted in the figures, C_{n_r} and C_{Y_β} have a negligible effect on the boundary. The effect of K_X on the branch of $R = 0$ which may be approximated by $D = 0$ is shown in figure 8. Complete calculations were made to obtain the $R = 0$ curves for the previously discussed free-flight airplane model. The value of A_2 used in these calculations was 0.17. For purposes of comparison, K_X was arbitrarily increased by a factor of 2.5. Again the results show practically no effect of K_X on this branch of $R = 0$, as is indicated by the simplified expression $D = 0$. For the case discussed in figures 6 to 8, the branch of $R = 0$ approximated by $R_1 = 0$ is in the second quadrant and has little practical importance. Hence, the effect of these parameters on R_1 was not determined for this particular case.

Effect of Product of Inertia on the Branches of $R = 0$ Approximated by $R_1 = 0$ and $E = 0$

The product of inertia has been shown to have a very pronounced effect on the lateral stability of present-day airplanes designed for high-speed high-altitude flight (references 1 and 7). The importance of the product of inertia is illustrated in figure 9(a), which presents the $R = 0$ boundaries of the hypothetical airplane discussed in reference 1 for two angles of inclination of the principal axis relative to the flight path, $\eta = 0^{\circ}$ and $\eta = 2^{\circ}$. Calculations were also made for these cases using $R_1 = 0$; and the results presented in figure 9(a) show the same marked stabilizing shift in the boundary, caused by the 2° inclination of the principal axis above the flight path, as obtained by the complete calculations. The value of A_2 for the $R_1 = 0$ calculations was −0.18. The value of C_{n_p} was then increased so that A_2 was equal to 0.13 (fig. 9(b)). In this case, $D = 0$ appears in the first quadrant and $R_1 = 0$ is in the second quadrant. Although both $D = 0$ and $R_1 = 0$ are valid boundaries, the results are discussed only for the effect of product of inertia on $D = 0$ since only the C_{n_β},C_{l_β} combinations in the first quadrant are usually of practical significance. Calculations for $\eta = 0^{\circ}$ and $\eta = 2^{\circ}$ were made using $D = 0$ and $R = 0$. Although the product-of-inertia factor K_{XZ} does appear in the D expression (in the term $-2C_LK_{XZ}$), an examination of D indicates that this term could have only a negligible effect on $D = 0$ when C_{l_p} is much greater than $2C_LK_{XZ}$, as is usually the case. Figure 9(b) shows that the results predicted from $D = 0$ agree very well with the results obtained from the complete calculations.

Effect of Radii of Gyration on the Branch of $R = 0$ Approximated by $R_1 = 0$

Figures 10 to 12 are presented for the purpose of showing the close agreement between results obtained by using $R_1 = 0$ and results obtained from reference 1. The three figures illustrate the effect of the radii of gyration in roll and yaw k_{X_0} and k_{Z_0}, respectively, on the neutral-oscillatory-stability boundary. Figure 12 emphasizes the fact that the simplified expression is sufficiently accurate to predict the effect of k_{X_0} on the oscillatory-stability boundary throughout the entire range of variation of k_{X_0}.

Effect of Wing Loading and Altitude on the Branches of $R = 0$

Approximated by $R_1 = 0$ and $D = 0$

The effects of wing loading and altitude on the neutral-oscillatory-stability boundaries were determined simultaneously by considering variations in the relative density factor μ_b because μ_b varies directly with both wing loading and altitude. An examination of the expressions $R_1 = 0$ and $D = 0$ indicated that increasing μ_b causes a slight destabilizing shift in $R_1 = 0$ but does not affect $D = 0$ since μ_b does not appear in the expression for $D = 0$. The trend shown by these results agrees with the results found in reference 1 concerning the effect of μ_b on the neutral-oscillatory-stability boundary.

Comparison between Neutral-Oscillatory-Stability Boundaries

Obtained by Exact and Simplified Expressions for a

High-Speed Experimental Airplane

Some of the neutral-oscillatory-stability boundaries obtained from recent calculations for several experimental high-speed airplanes have appeared much different from the conventional stability boundaries. Because of the complexity of the complete expression for $R = 0$, it is difficult to determine the reasons for such unusual looking curves and the significance of the boundaries. From the simplified expressions, however, a complete analysis of the boundaries can be easily obtained. The $R = 0$ boundaries of an experimental airplane are shown in figure 13(a). In addition to the $R = 0$ boundaries, the $D = 0$ boundaries are also plotted in the figure. As mentioned at the outset of the paper, $R = 0$ is a neutral-oscillatory-stability boundary only if D is positive. The $R = 0$ boundaries on the hatched side of $D = 0$ are not therefore neutral-oscillatory-stability boundaries. The boundaries for the same experimental airplane calculated from the simplified expressions are plotted in figure 13(b). The $R_1 = 0$ and $D = 0$ boundaries which are not neutral-oscillatory-stability boundaries, as determined by the analysis presented in the section entitled "Validity of $D = 0$ and $R_1 = 0$ as Neutral-Oscillatory-Stability Boundaries," are shown as dash-line curves in the figure. In $D = 0$, the coefficient of C_{l_β} becomes zero at $C_{n_\beta} = 0.056$ and, therefore, the $D = 0$ boundary approaches positive infinity in the second quadrant at $C_{n_\beta} = 0.056$. As C_{n_β} increases above 0.056, $D = 0$ returns from negative infinity and appears in the first quadrant. Similarly, $R_1 = 0$ approaches negative infinity when C_{n_β} is approximately equal to 0.25 since the coefficient of C_{l_β} in $R_1 = 0$ $\left(A_1K_{XZ} - A_2A_3\right)$ is zero at this value of C_{n_β}. Above C_{n_β} of 0.25, $R_1 = 0$ returns from positive infinity and appears in the second quadrant. It is necessary to note that in figure 13(a) the neutral-oscillatory-stability boundary is one continuous curve; whereas in figure 13(b) this boundary is composed of two sections, one section of $R_1 = 0$ and the other section of $D = 0$. The latter fact provides the important information that the period of the oscillation which becomes unstable upon passing through the $D = 0$ boundary is comparatively longer than the period of the oscillation which becomes unstable upon passing through the $R_1 = 0$ boundary.

CONCLUSIONS

The following conclusions were reached from a theoretical investigation of a simplified method for obtaining and analyzing the neutral-lateral-oscillatory-stability boundary:

1. A necessary condition for the lateral-neutral-oscillatory-stability boundard is that $R = D(BC - AD) - B^2E = 0$, where A, B, C, D, and E are the coefficients of the lateral-stability equation. The expression for $R = 0$ is approximated by the expressions $D = 0$ and $R_1 = BC - AD = 0$. Criterions are derived which, if satisfied, indicate that the approximate expressions satisfy the necessary and sufficient conditions for a neutral-oscillatory-stability boundary.

2. If $D = 0$ and $R_1 = 0$ approximate $R = 0$, the curve $D = 0$ represents the neutral-oscillatory-stability boundary for the oscillation which has a period comparatively longer than the period of the oscillation for which $R_1 = 0$ is the boundary.

3. In general, the results of the computations obtained from $R_1 = 0$ and $D = 0$ show very good agreement with the results calculated by the exact expression for $R = 0$. Specifically, the results of the investigation indicated:

(a) An increase in the absolute value of the parameter A_2, which is equal to $C_{n_p} - 2C_L K_Z^2$ (where C_{n_p} is the yawing-moment coefficient due to rolling-angular-velocity factor, C_L is the trim lift coefficient, and K_Z is the radius of gyration in yaw) causes a destabilizing shift in the branches of $R = 0$ approximated by $D = 0$ and $R_1 = 0$.

(b) The branch of $R = 0$ approximated by $D = 0$ mainly depends upon the parameter A_2 and the damping-in-roll derivative C_{l_p}. The product-of-inertia term K_{XZ} also appears in D, but it has a negligible effect on the branch of $R = 0$ approximated by $D = 0$.

(c) An increase in the relative-density factor μ_b causes a destabilizing shift on the branch of $R = 0$ approximated by $R_1 = 0$ but does not affect the branch of $R = 0$ approximated by $D = 0$.

4. The neutral-oscillatory-stability boundaries computed from the simplified expressions show excellent agreement with the corresponding boundaries presented in NACA TN No. 1282.

Langley Aeronautical Laboratory
National Advisory Committee for Aeronautics
Langley Field, Va., August 4, 1948

APPENDIX A

DERIVATION OF TEST FUNCTIONS Δr AND Δd

For a given value of C_{n_β}, selected from the probable range of C_{n_β} of the airplane for which the lateral-stability analysis is to be made, let

$$R_1 = r_1 C_{l_\beta} + r_2 \qquad \frac{\partial R_1}{\partial C_{l_\beta}} = r_1 \qquad \left(C_{l_\beta}\right)_{R_1=0} = \frac{-r_2}{r_1} = r$$

$$D = d_1 C_{l_\beta} + d_2 \qquad \frac{\partial D}{\partial C_{l_\beta}} = d_1 \qquad \left(C_{l_\beta}\right)_{D=0} = \frac{-d_2}{d_1} = d$$

$$B^2E = e_1 C_{l_\beta} + e_2 \qquad \frac{\partial B^2E}{\partial C_{l_\beta}} = e_1 \qquad \left(C_{l_\beta}\right)_{B^2E=0} = \frac{-e_2}{e_1} = e$$

As shown in figure 14 the exact roots of $R = R_1D - B^2E = 0$ occur at the intersection of the straight line B^2E with the parabola R_1D. In the vicinity of the point $C_{l_\beta} = r$, at which $R_1 = 0$, the curve R_1D is approximated well by a straight line tangent to the curve at $C_{l_\beta} = r$, that is,

$$R_1D \approx \left(\frac{\partial R_1 D}{\partial C_{l_\beta}}\right)_{R_1=0} \left(C_{l_\beta} - r\right) = \left(-r_2 d_1 + r_1 d_2\right)\left(C_{l_\beta} - r\right)$$

If there is a root of $R = R_1D - B^2E = 0$ near $R_1 = 0$ (that is, if B^2E intersects R_1D near the point r, in fig. 14) then

$$R = \left(-r_2 d_1 + r_1 d_2\right)\left(C_{l_\beta} - r\right) - e_1 C_{l_\beta} - e_2 = 0$$

Thus, the approximate deviation of a root of $R = 0$ from $R_1 = 0$ is given by

$$\Delta r \equiv \left(C_{l_\beta} - r\right) = \frac{r_1 e_2 - r_2 e_1}{r_1\left(r_1 d_2 - r_2 d_1 - e_1\right)}$$

$$= \frac{e_1(e - r)}{r_1 d_1(d - r) + e_1} \qquad \text{(A1)}$$

If this deviation, Δr, is small, then $R_1 = 0$ is a close approximation to one branch of $R = 0$. A suitable criterion for this approximation is

$$\left|\Delta r\right| \leqq \left|\frac{r}{5}\right|$$

or

$$\left|\Delta r\right| \leqq 0.01$$

whichever is the larger.

In the case of $D = 0$, a similar analysis results in the test function

$$\Delta d = \frac{e_1(e - d)}{r_1 d_1(r - d) + e_1} \qquad \text{(A2)}$$

If Δd is small, $D = 0$ may then be considered a close approximation to the other branch of $R = 0$. A suitable criterion for this approximation is

$$\left|\Delta d\right| \leqq \left|\frac{d}{5}\right|$$

or

$$\left|\Delta d\right| \leqq 0.01$$

whichever is the larger.

The expressions for r_1, d_1, and e_1 for use in equations (A1) and (A2) are

$$r_1 = 8\mu_b\left(A_1K_{XZ} - A_2A_3\right)$$

$$d_1 = \mu_bA_2$$

$$e = 2\mu_bA_1{}^2C_LC_{n_r}$$

where

$$A_1 = K_X{}^2C_{n_r} + 2K_X{}^2K_Z{}^2C_{Y_\beta} + C_{l_p}K_Z{}^2$$

$$A_2 = C_{n_p} - 2C_LK_Z{}^2$$

$$A_3 = K_X{}^2K_Z{}^2 - K_{XZ}{}^2$$

REFERENCES

1. Sternfield, Leonard: Some Considerations of the Lateral Stability of High-Speed Aircraft. NACA TN No. 1282, 1947.

2. Johnson, Joseph L., and Sternfield, Leonard: A Theoretical Investigation of the Effect of Yawing Moment due to Rolling on Lateral Oscillatory Stability. NACA TN No. 1723, 1948.

3. Routh, Edward John: Dynamics of a System of Rigid Bodies. Part II. 6th ed., rev. and enl., Macmillan and Co., Ltd. (London), 1905, p. 223.

4. Dickson, Leonard Eugene: Elementary Theory of Equations. John Wiley & Sons, Inc., 1917, pp. 38–45.

5. Jones, Robert T.: A Simplified Application of the Method of Operators to the Calculation of Disturbed Motions of an Airplane. NACA Rep. No. 560, 1936.

6. Jones, Robert T.: Calculation of the Motion of an Airplane under the Influence of Irregular Disturbances. Jour. Aero. Sci., vol. 3, no. 12, Oct. 1936, pp. 419–425.

7. Sternfield, Leonard: Effect of Product of Inertia on Lateral Stability. NACA TN No. 1193, 1947.

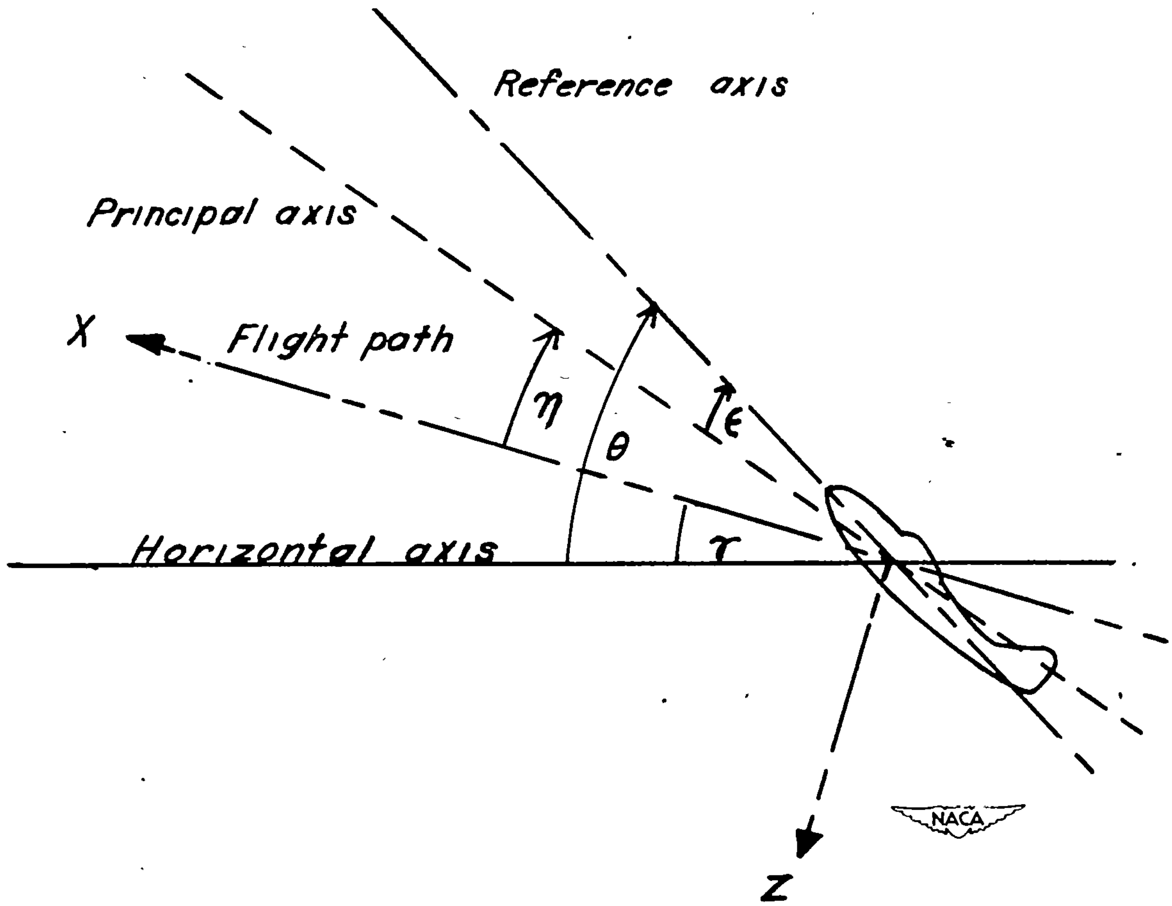

Figure 1.- System of axes and angular relationships in flight. Arrows indicate positive direction of angles. $\eta = \theta - \gamma - \epsilon$.

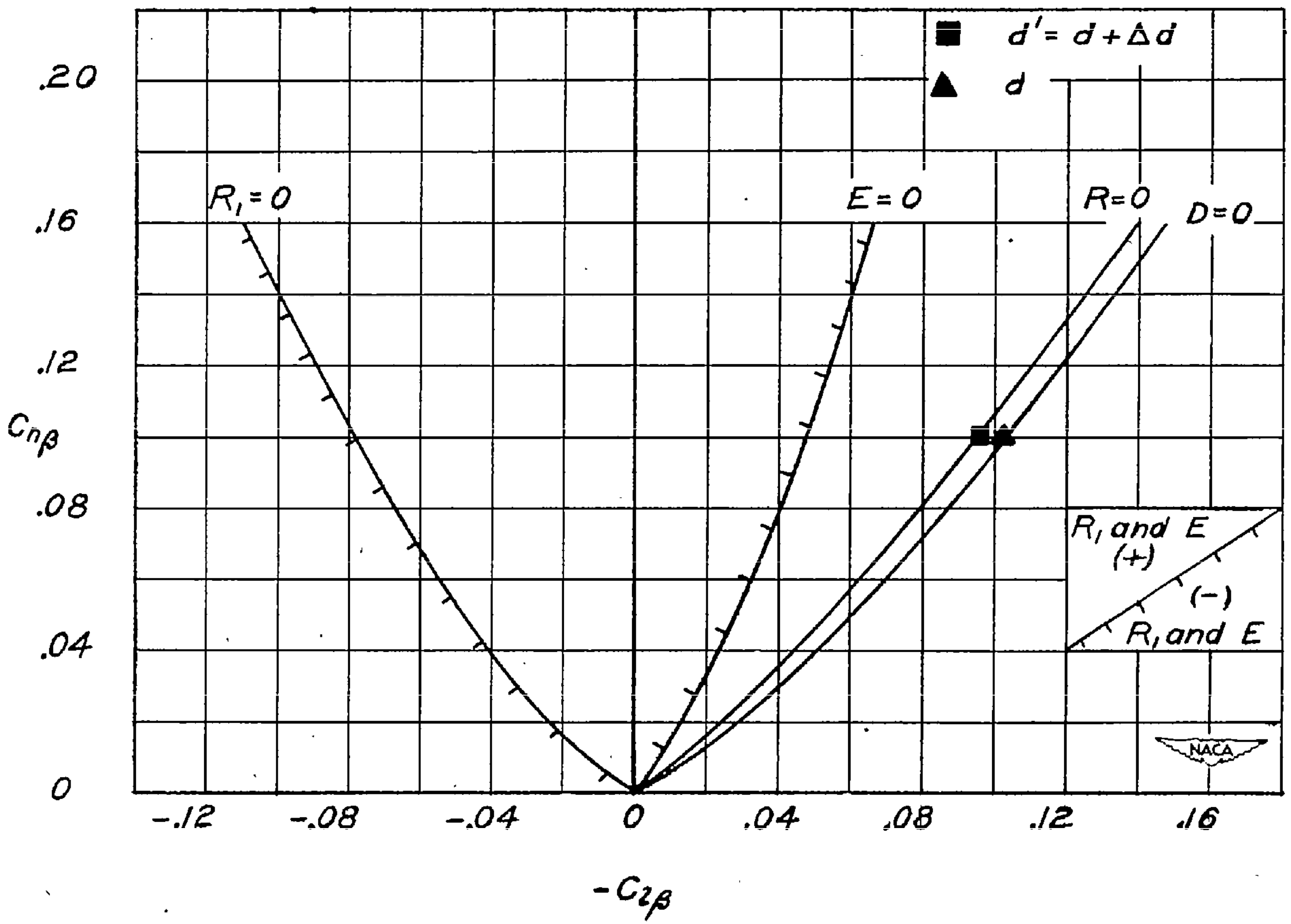

Figure 2.- Validity of D = 0 as a neutral-oscillatory-stability boundary.

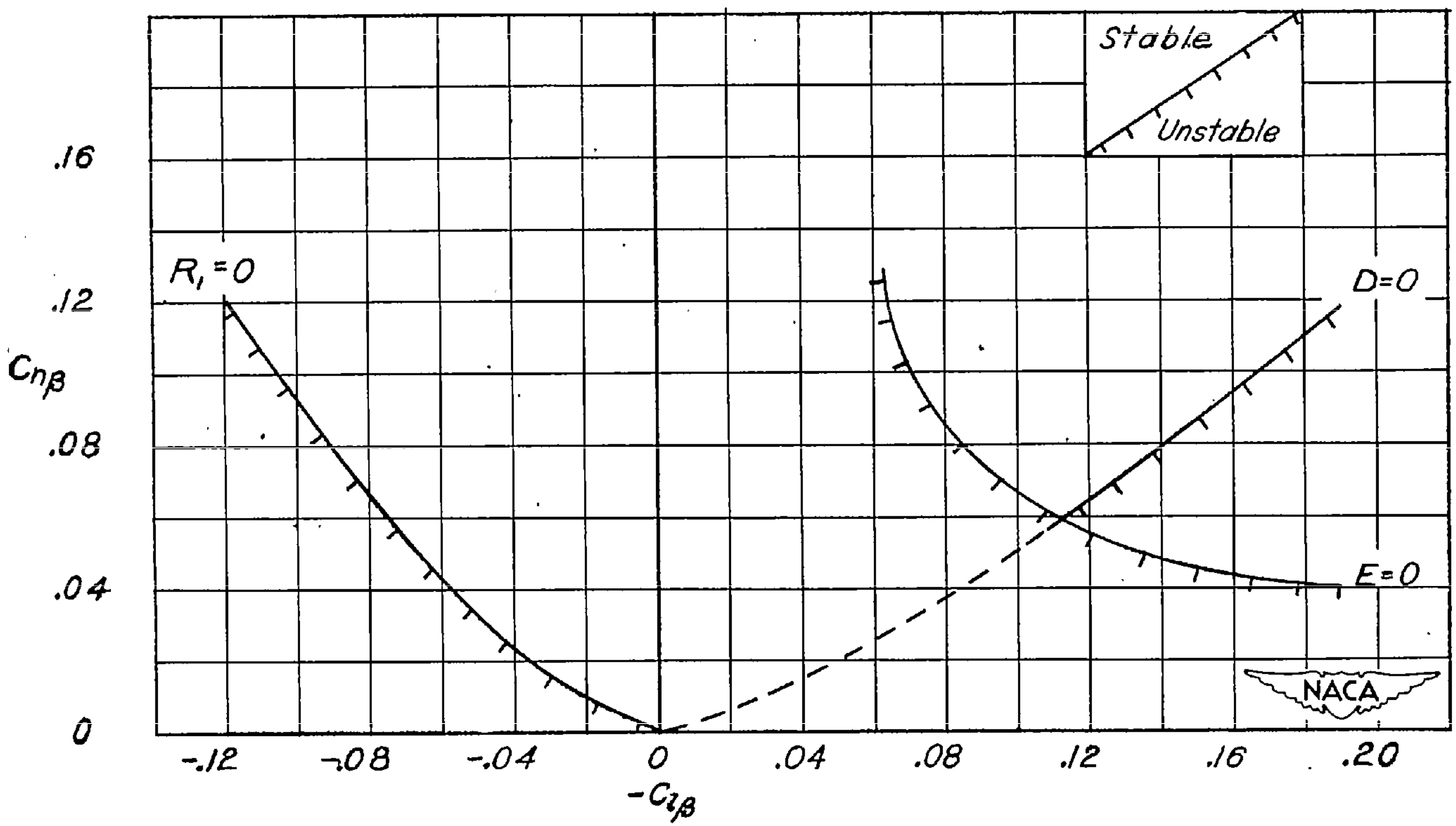

Figure 3.- Effect of the position of the E = 0 boundary on the validity of D = 0 as an approximate neutral-oscillatory-stability boundary.

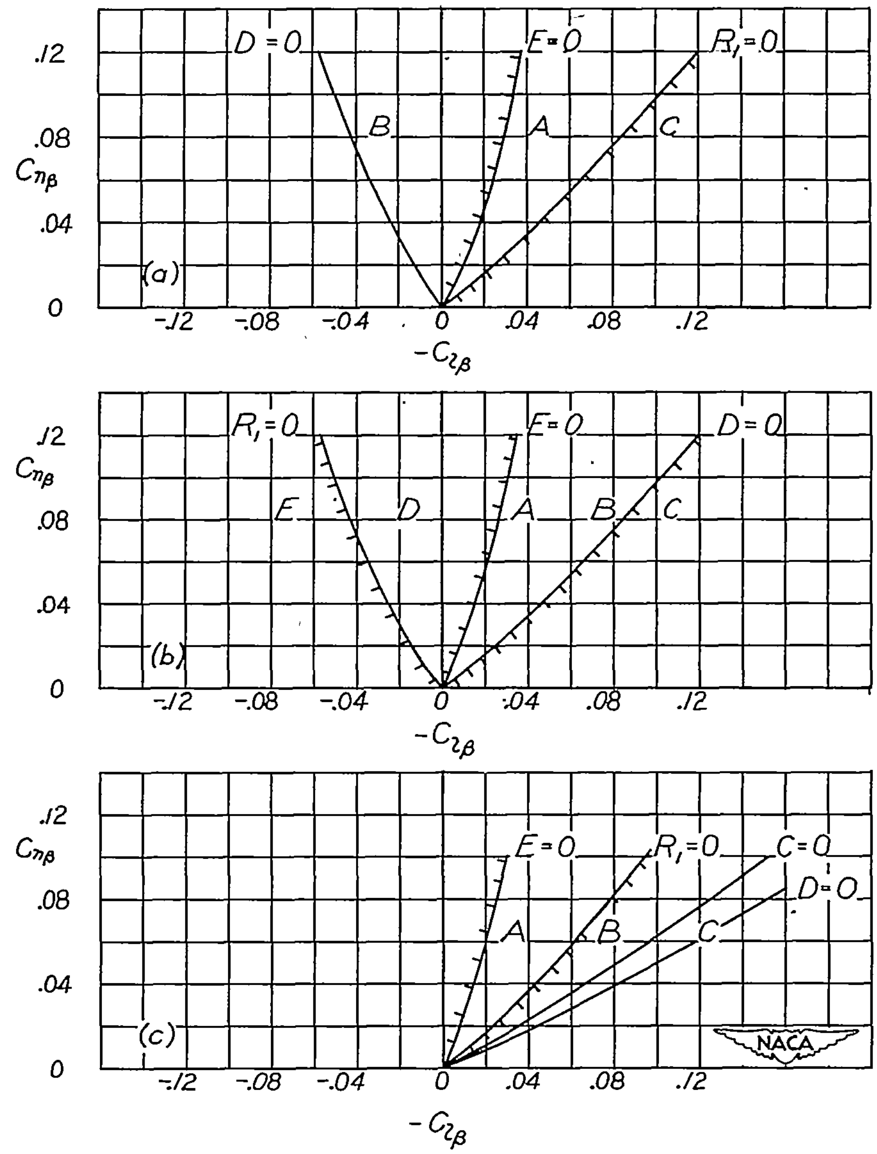

Figure 4.- Nature of roots of stability equation in C_{n_β}, C_{l_β} plane.

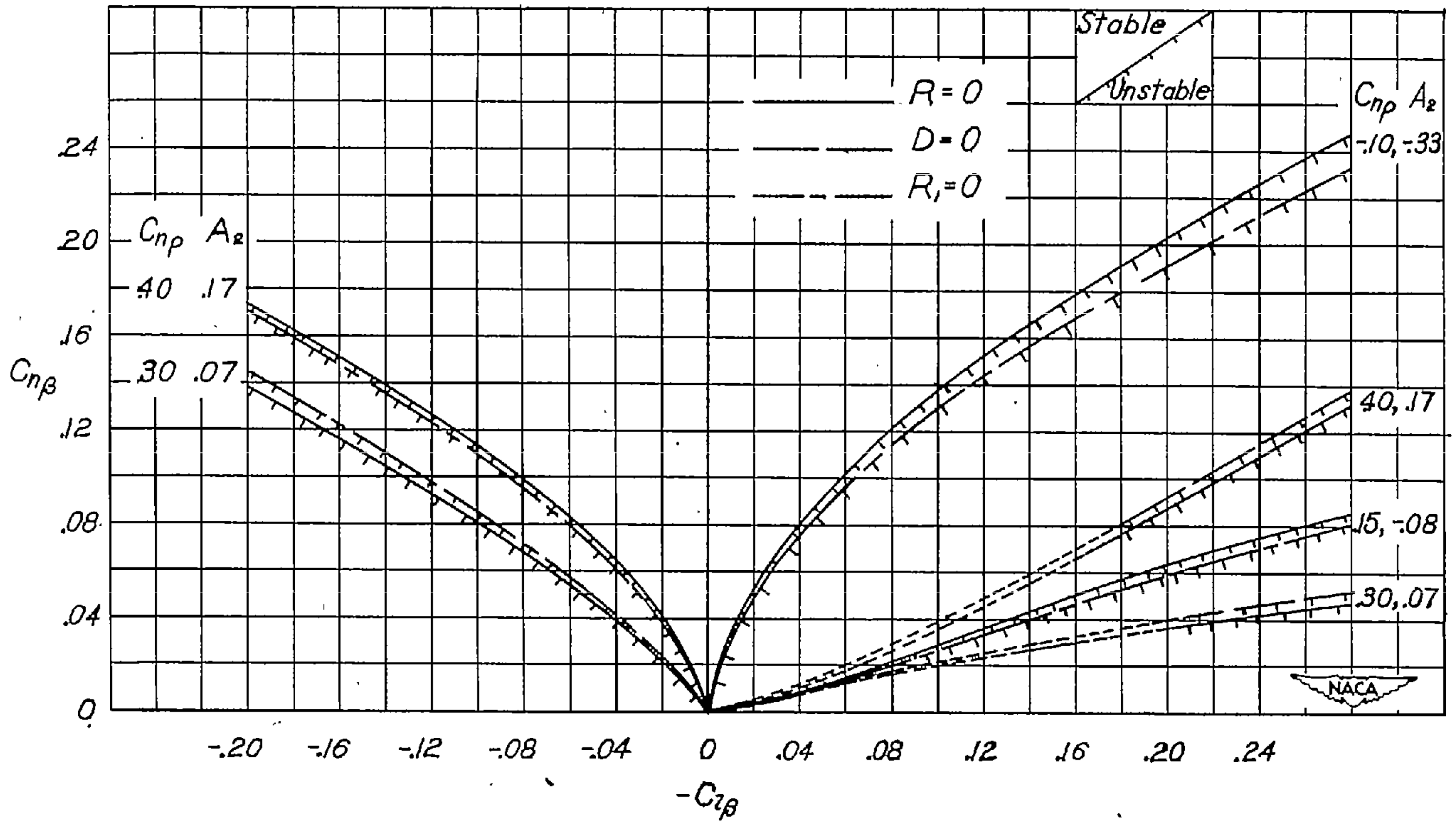

Figure 5.- Effect of C_{n_p} and A_2 on the neutral-oscillatory-stability boundary.

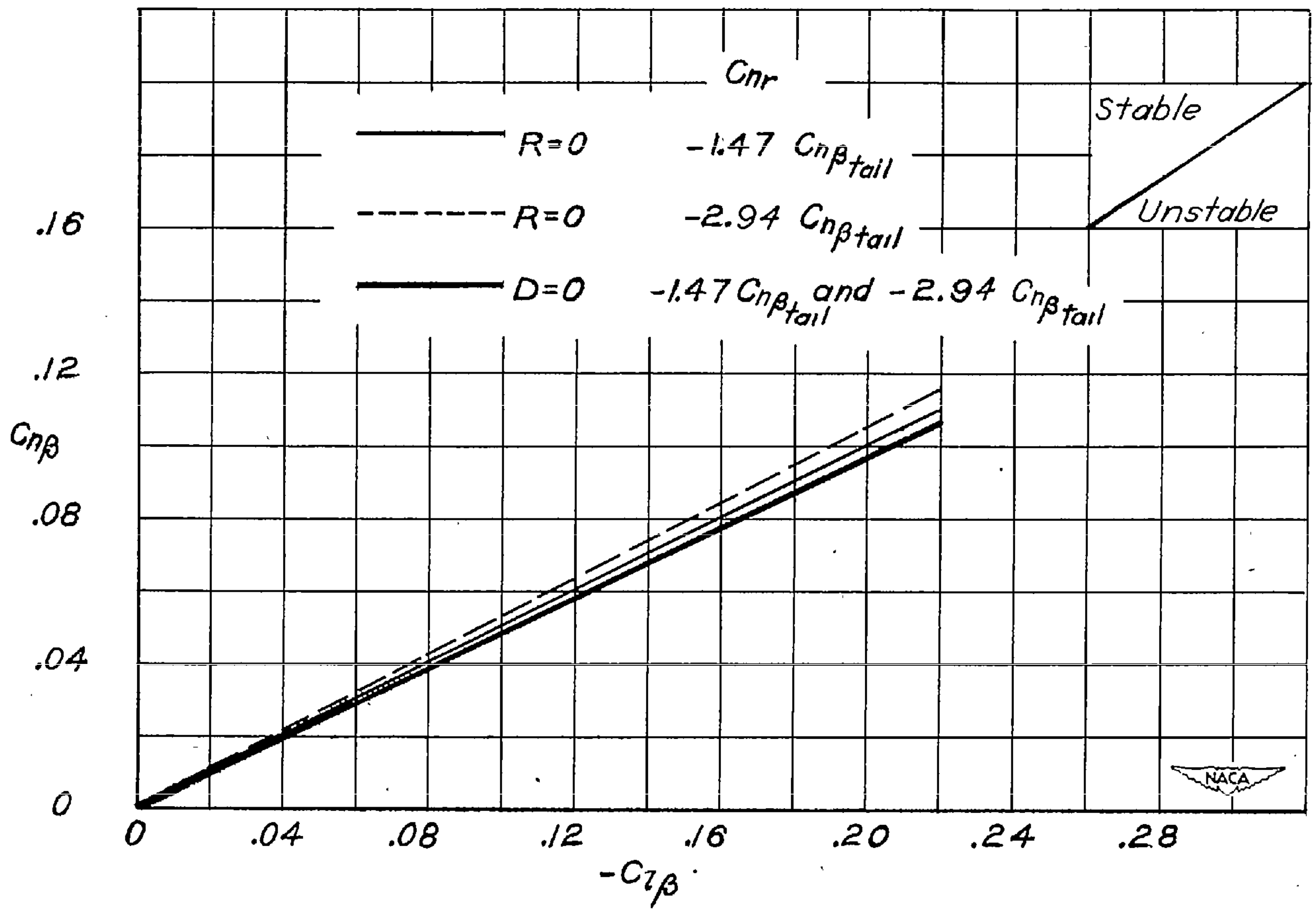

Figure 6.- Effect of C_{n_r} on the neutral-oscillatory-stability boundary.

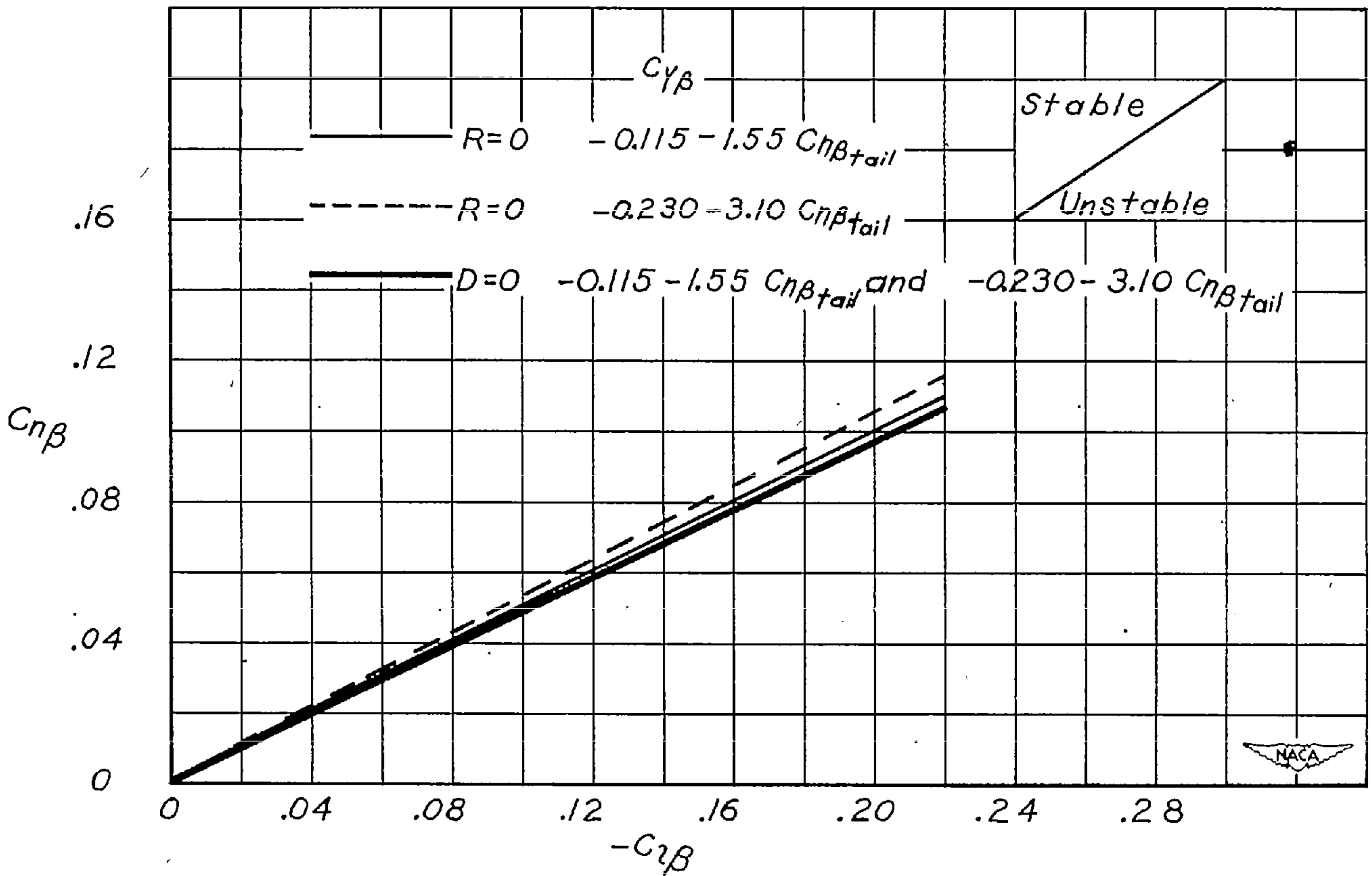

Figure 7.- Effect of C_{Y_β} on the neutral-oscillatory-stability boundary.

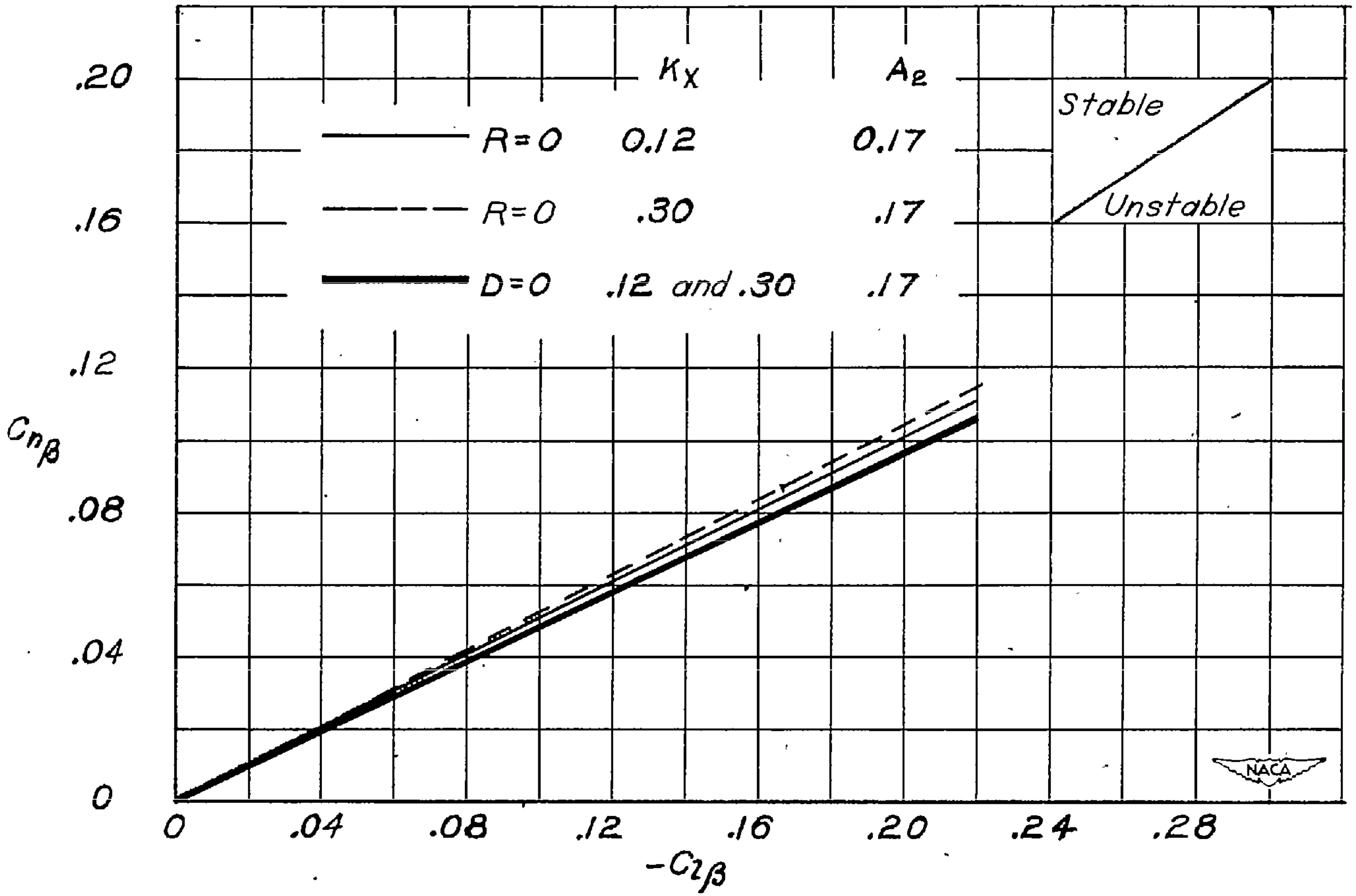

Figure 8.- Effect of K_X on the neutral-oscillatory-stability boundary.

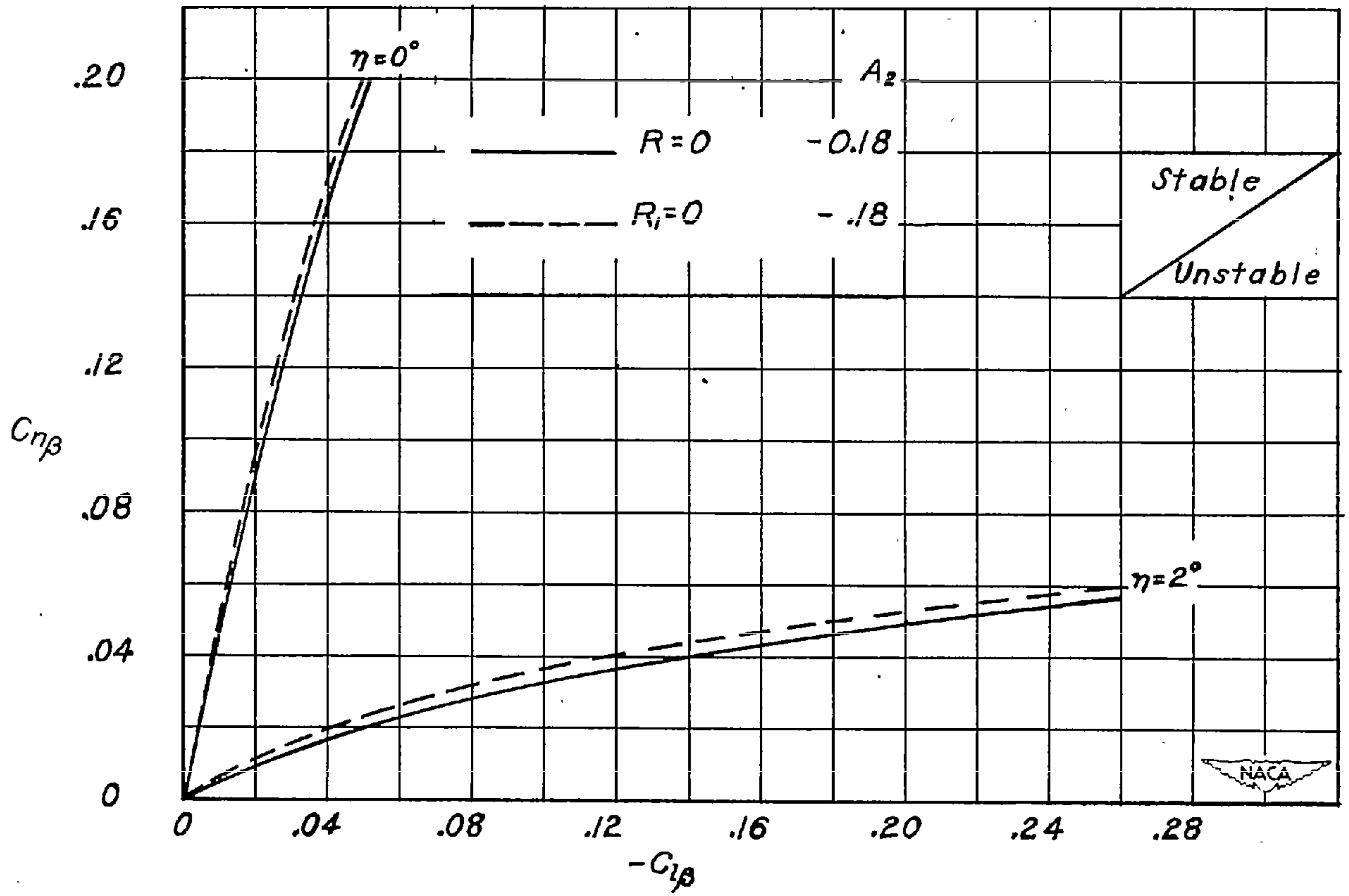

(a) Negative A_2.

Figure 9.- Effect of K_{XZ} on the neutral-oscillatory-stability boundary.

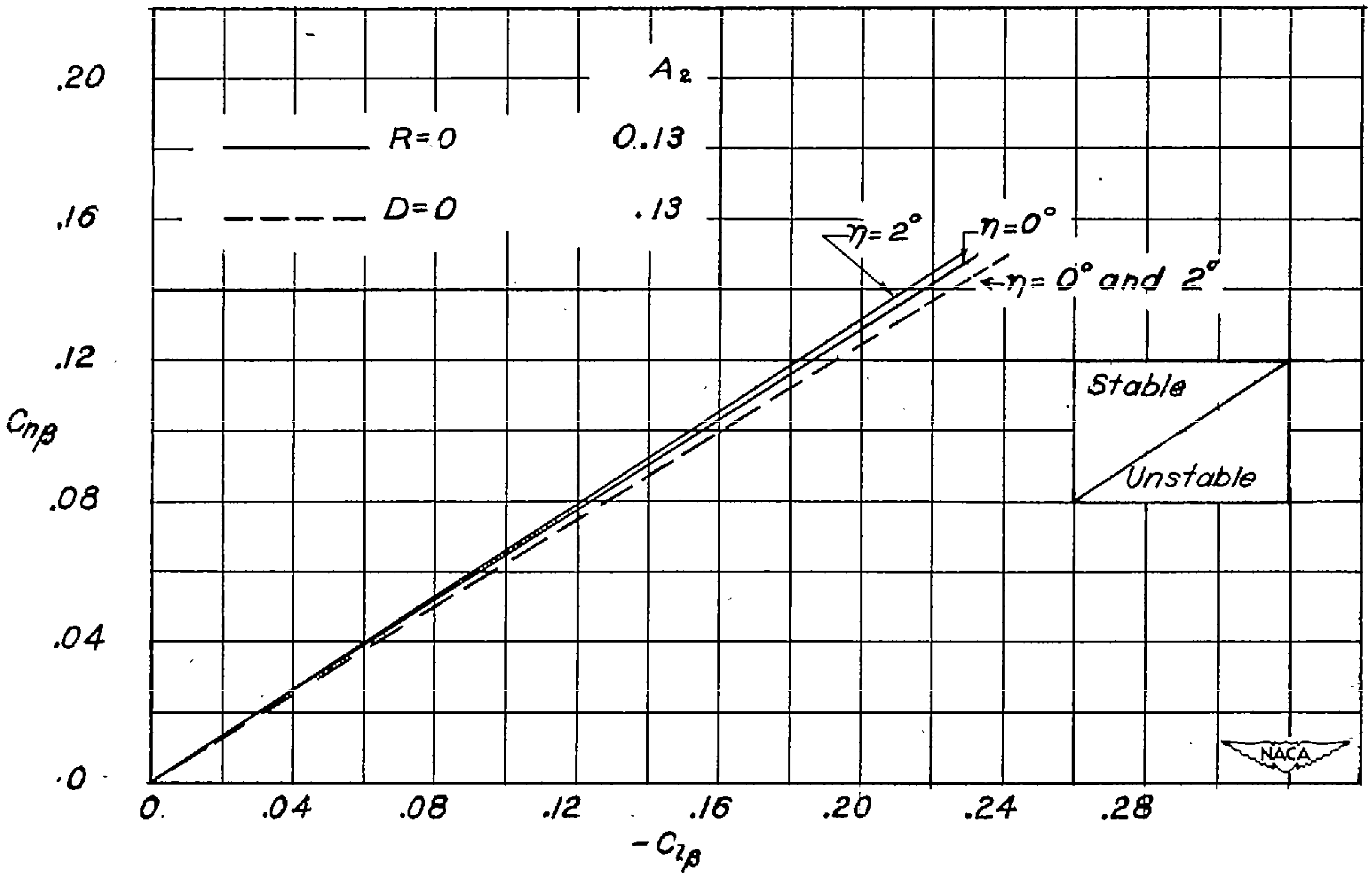

(b) Positive A_2.

Figure 9.- Concluded.

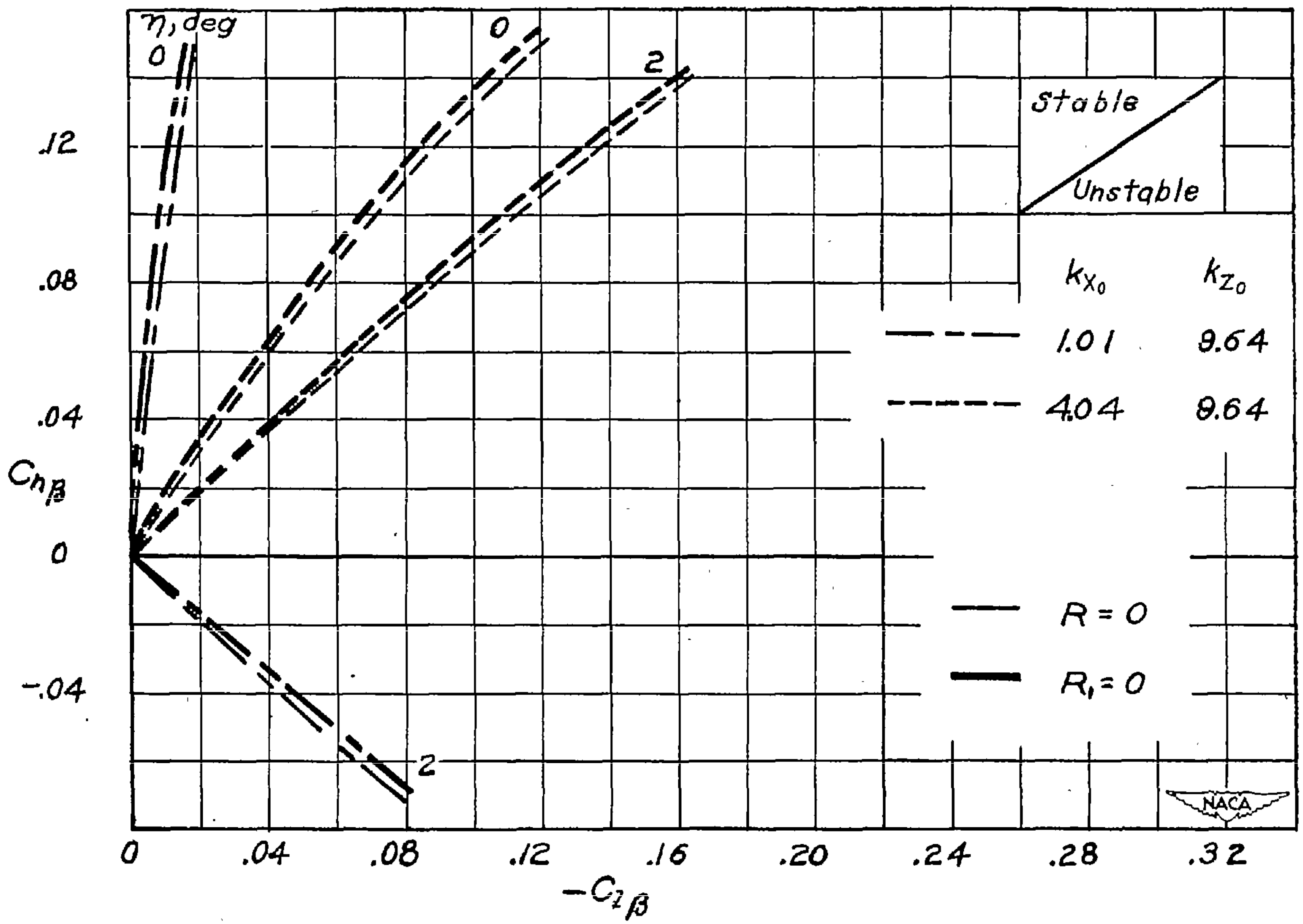

Figure 10.- Effect of k_{X_0} on the neutral-oscillatory-stability boundary.

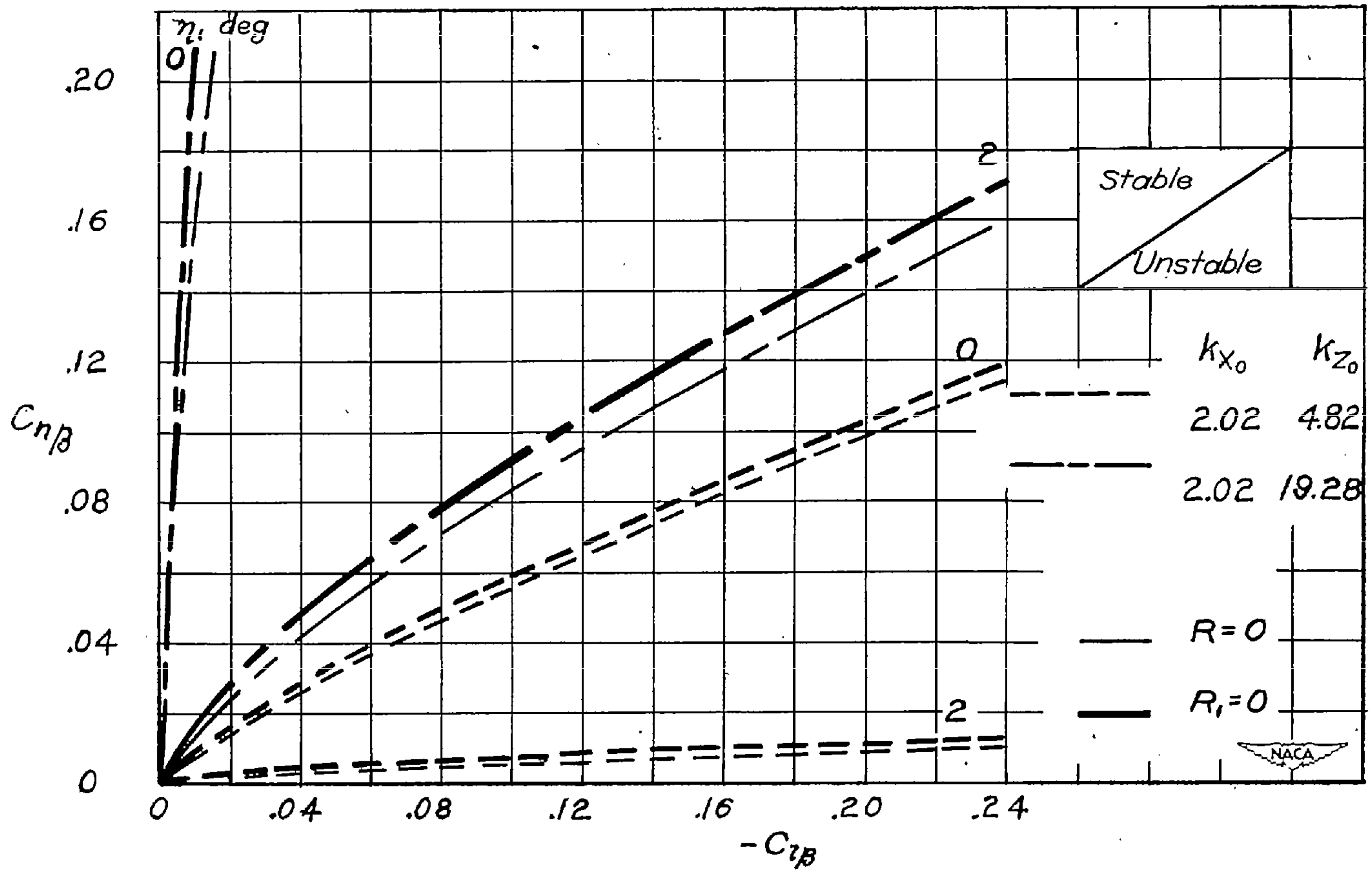

Figure 11.- Effect of k_{Z_0} on the neutral-oscillatory-stability boundary.

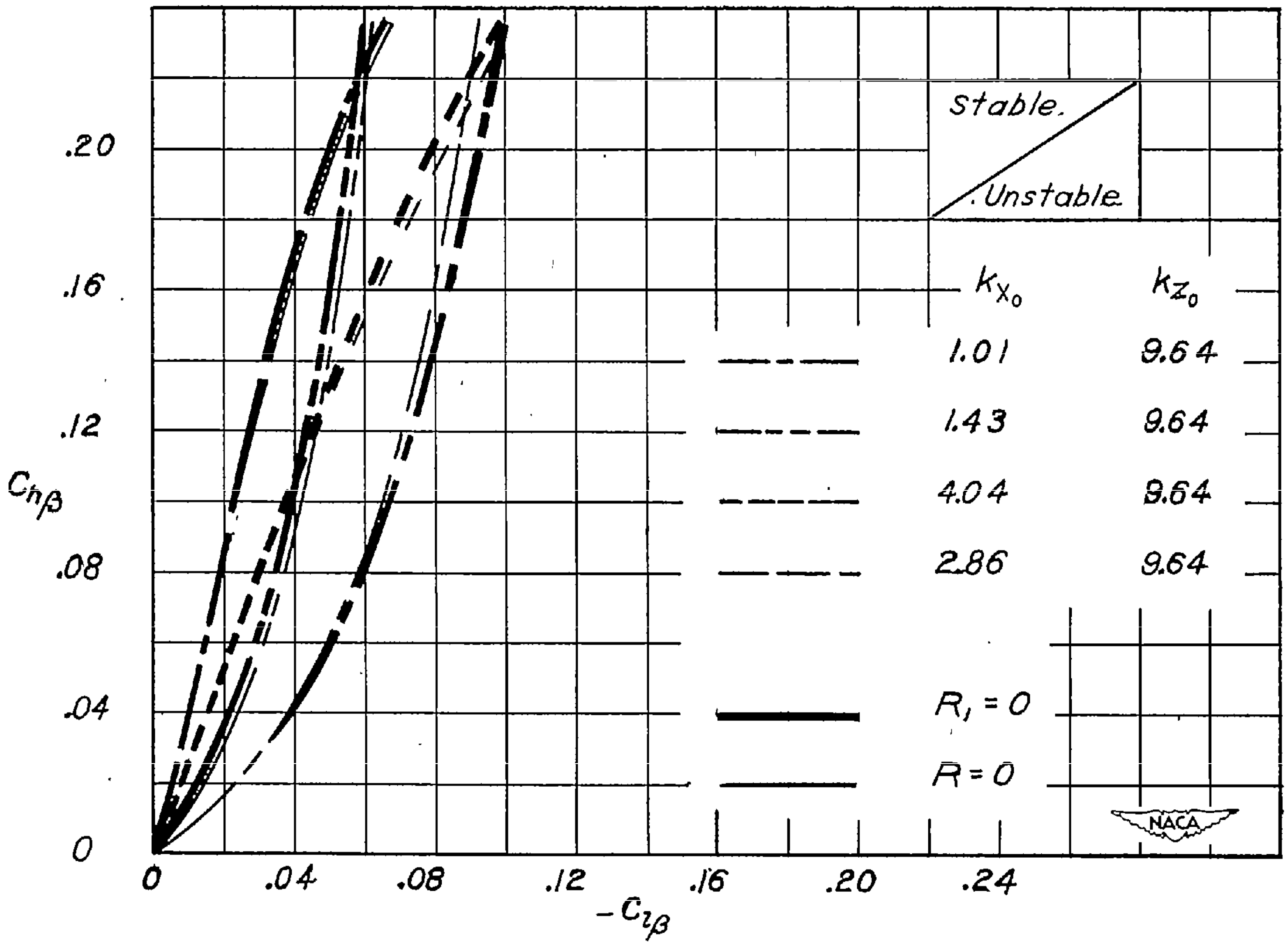

Figure 12.- Effect of k_{X_0} on the neutral-oscillatory-stability boundary.

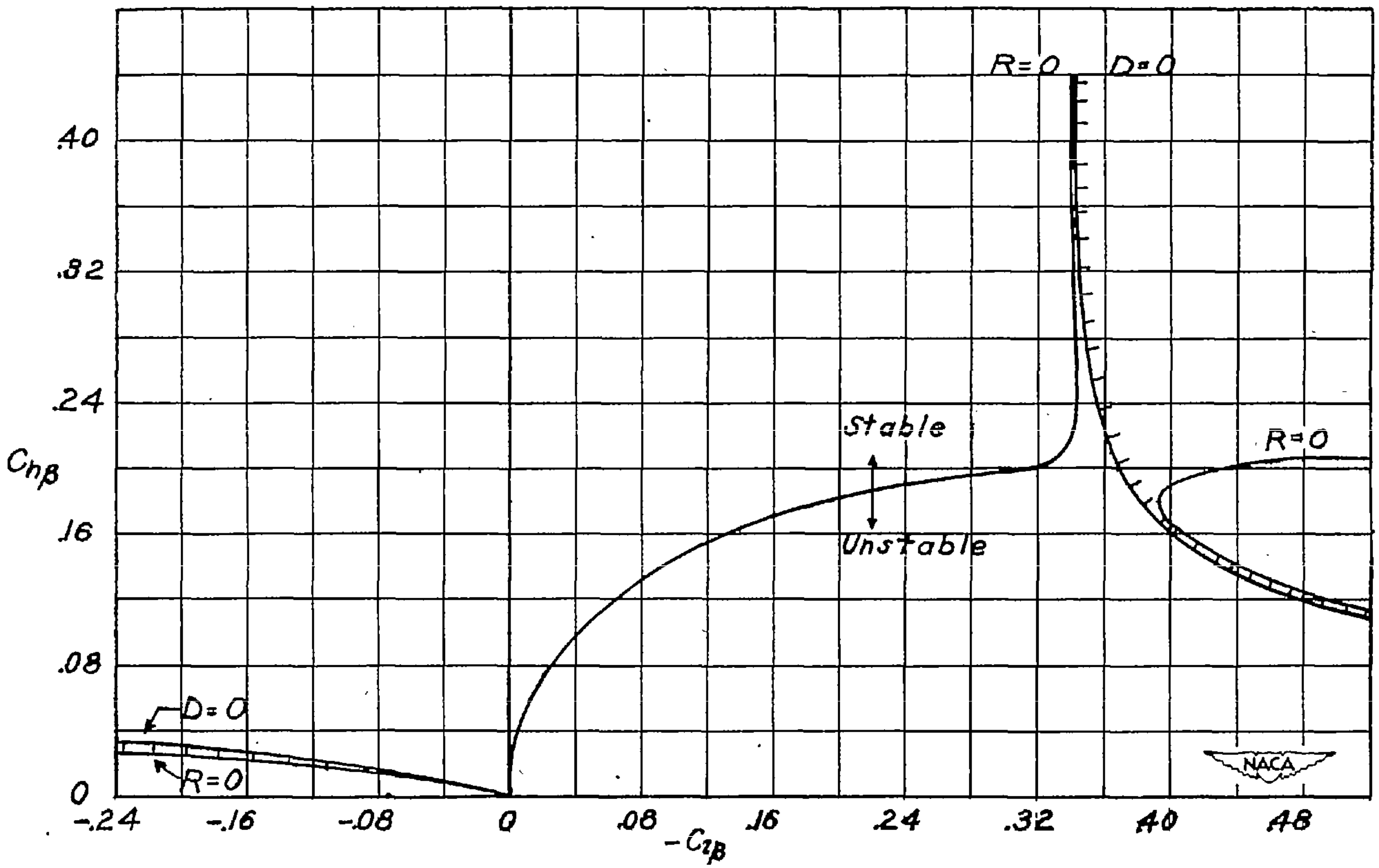

(a) $R = R_1D - B^2E = 0.$

Figure 13.- Oscillatory stability boundaries for an experimental high-speed airplane.

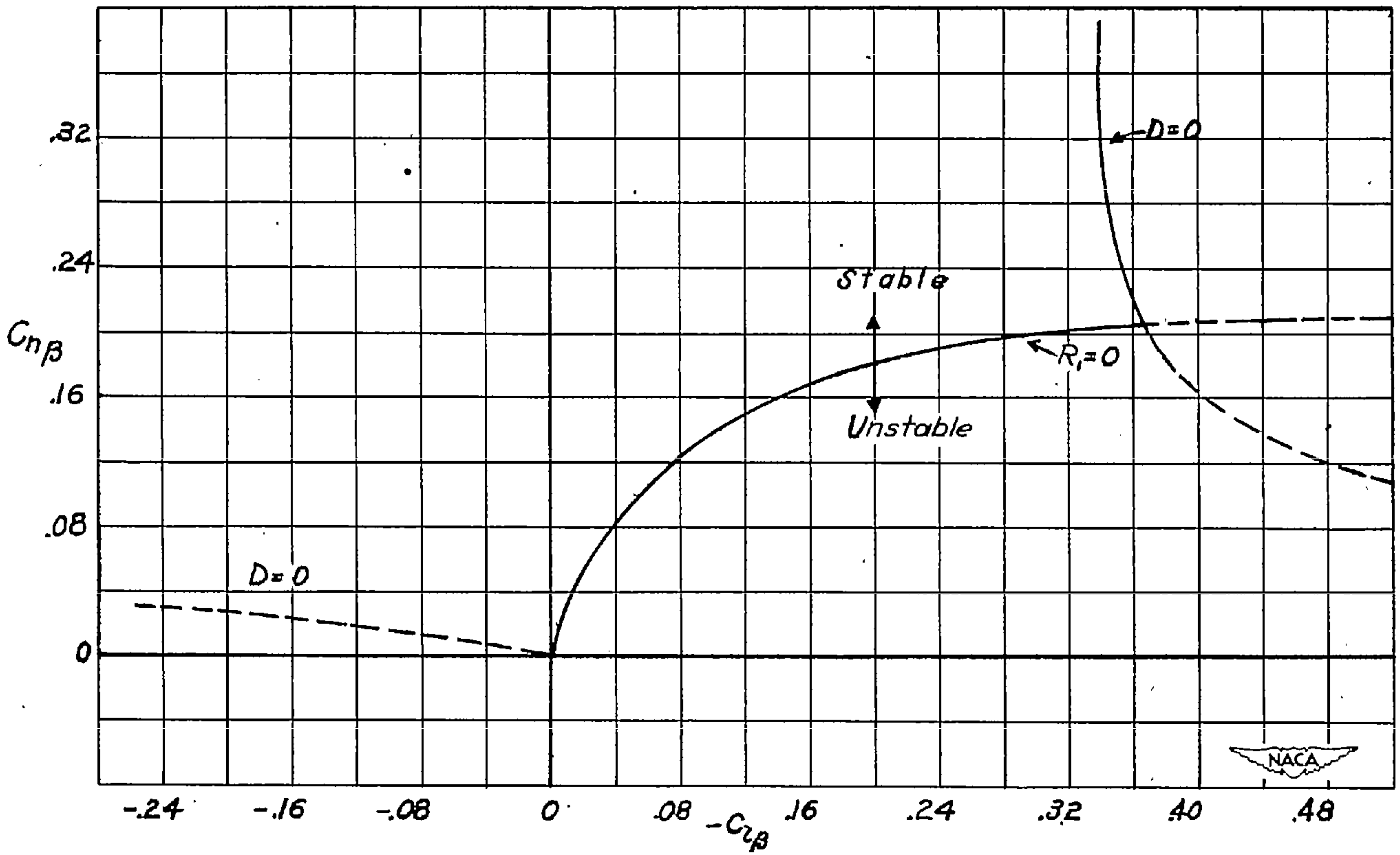

(b) $R_1 = 0$ and $D = 0$.

Figure 13.- Concluded.

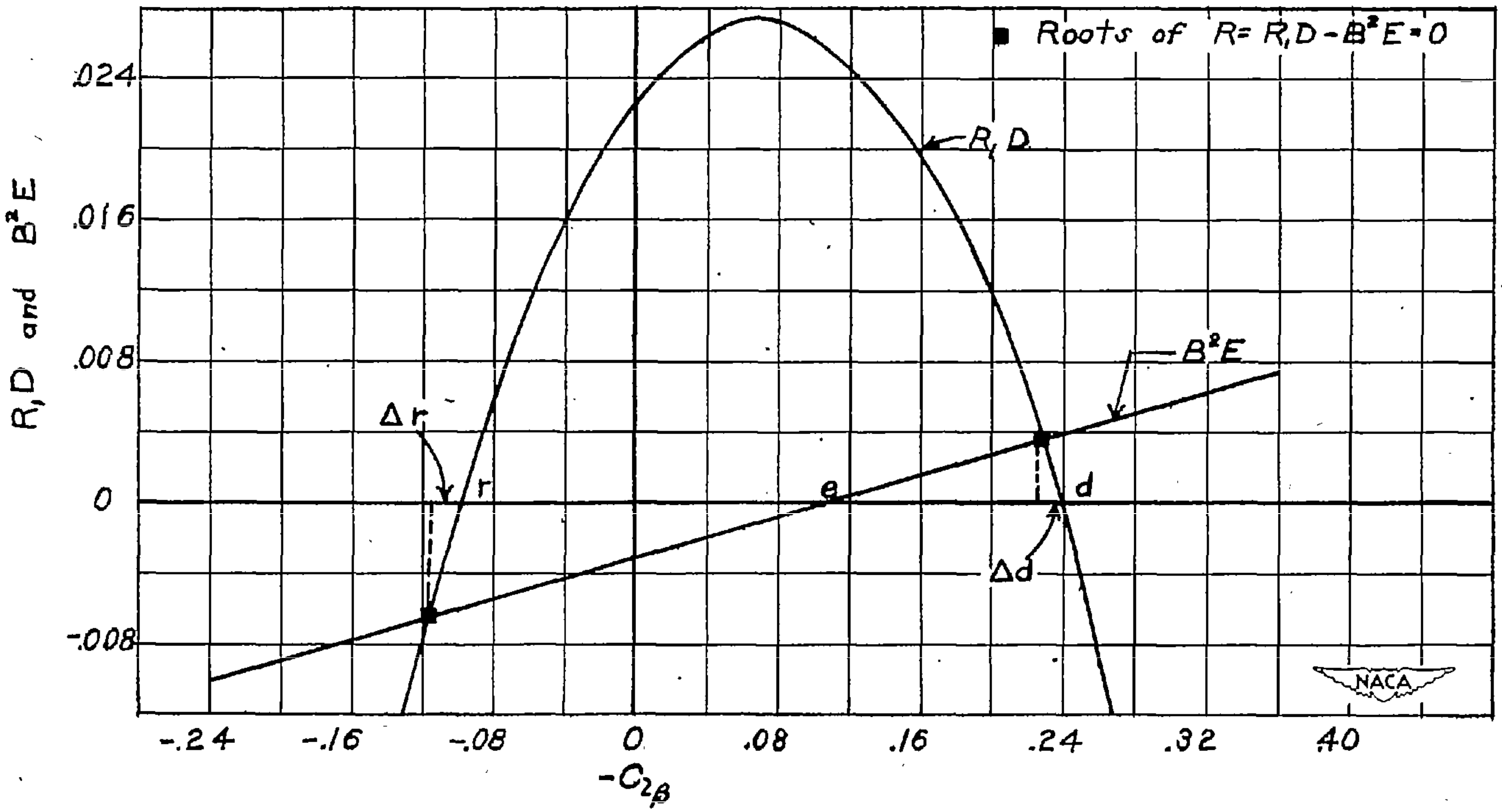

Figure 14.- Graphical representation of the roots of the $R = 0$ boundary.